Hydraulics Research
Wallingford

CALIBRATION OF WAVE TRANSFORMATION COMPUTER MODELS AGAINST FIELD DATA

C E Jelliman B.Sc

Report SR 194
March 1989

Registered Office: Hydraulics Research Limited, Wallingford, Oxfordshire OX10 8BA.
Telephone: 0491 35381. Telex: 848552

This report describes work carried out by Hydraulics Research under Commission 14D2 funded by the Ministry of Agriculture, Fisheries and Foods, whose nominated officer was Mr A J Allison. At the time of reporting this project, Hydraulics Research's nominated project officer was Dr S W Huntington.

DRAFT

ABSTRACT

This report describes a calibration of wave transformation programs developed by Hydraulics Research Limited. A brief literature review and data search for potential sites was carried out. The calibration concentrated on wave data recorded at Perranporth on the north coast of Cornwall. The storms with highest wave heights were chosen from the recording period which was 10 months long over the winter of 1978/1979. A wave hindcasting model was used to predict offshore directional spectra for the 26 storms using wind records.

Models of varying complexity were used to transform them to the inshore location. These included the OUTRAY back-tracking ray model and the Nearshore Profile Model. The results were compared with the measured data.

All the computer models included refraction and shoaling. One model had the option of including the effects of breaking and friction. Wave breaking was shown to be negligible at this site but seabed friction did have some effect.

The results closest to the measured values were predicted by the OUTRAY model. On average this model over-predicted the inshore wave heights by 1.7% and the wave periods by 2.7%. The other models over-predicted the wave heights by 6% and the wave periods by 5.7 to 8.7%. Unlike the OUTRAY model, they represent the seabed using parallel contours which are orientated by supplying a beach normal. The results from these models were shown to be dependent on the accuracy of this beach normal.

The work described in this report was sponsored by the Ministry of Agriculture, Fisheries and Food.

For further details on this report please contact Miss C E Jelliman or Dr A H Brampton of the Maritime Engineering Department, headed by Dr S W Huntington.

CONTENTS

CONTENTS (CONT'D)

FIGURES (CONT'D)

APPENDICES

1 INTRODUCTION

Hydraulics Research Limited (HR) have many different computer models of varying complexity for transforming offshore wave conditions into conditions at a given inshore location. These include models based on finite difference, back-tracking and forward-tracking ray projection methods. Some include the effects of seabed friction, wave breaking, currents and diffraction around breakwaters and headlands. The aim of this study was to calibrate some of these models against field data.

1.1 Outline of report

This chapter describes the choice of site and models for use in this calibration study. Chapter 2 gives a brief description of each of the models. Calibration of the models at a specific site and the results are described in Chapter 3. A discussion about the results obtained from this study and about the range of applicability of the models is given in Chapter 4. Finally the conclusions from this study are given in the last chapter.

1.2 Choice of models

The wave transformation model most frequently used at HR is the OUTRAY model. This is a back-tracking ray projection wave refraction model which uses a set of depth grids to represent the seabed. This model is generally cheaper to use than finite difference and forward-tracking models if results are required at only one inshore position. OUTRAY produces a wave transformation matrix for a given location and water level which can be used to transform many wave spectra. Finite difference and forward tracking models usually require a run of the model for each offshore spectrum or even each frequency component of the spectrum.

A simplified version of the OUTRAY model has been developed which assumes a parallel contoured seabed with constant slope. This is known as the Parallel Contour Model (PCM). This has only been used at a few sites where the contours appeared to be virtually straight and parallel and/or a quick inexpensive approximation of inshore conditions was required.

The Nearshore Profile Model (NPM) is a model for predicting wave and current interaction but it can be used ignoring the effects of current if required. It assumes parallel contours like the PCM. It calculates values at points along a cross-section of the seabed normal to the contours. Unlike the OUTRAY model and PCM, this model has to be run for each offshore wave spectrum. The NPM can include the effects of seabed friction and wave breaking if required.

The above three models were used in this calibration study. Further models may be calibrated in future studies.

1.3 Choice of site

For an accurate calibration of a wave transformation model to be possible, accurate offshore and inshore field data must be available. None of the three models have been calibrated before using both offshore and inshore measured data. The PCM has never been calibrated with field data and the NPM has only been validated with tidal currents (Ref 1).

The OUTRAY model has been calibrated at inshore sites using predicted offshore wave conditions. These previous studies are listed in Table 1 along with references. The offshore wave conditions were predicted using the HR HINDWAVE model which hindcasts waves from wind data. These conditions were then refracted into the inshore point. The HINDWAVE model

was calibrated by comparing inshore predicted and measured wave data. The final results show how good HINDWAVE and OUTRAY can be together but would not necessarily give an indication of how good either one is on its own.

The second part of Table 1 lists the sites where simultaneous wave data has been recorded both offshore and at one or more sites inshore. Further details about the measured wave data are given in Reference 21.

There are ten possible sites with data that could be used to calibrate the models. The data for Lowestoft, Great Yarmouth, Haringvliet and Sylt is not owned by HR and the availability of it was not known. Two of the other six sites, Falmouth and South Uist, have a seabed which is uneven. Non-linear effects such as seabed friction are likely to be important at these sites but the OUTRAY model and PCM do not include these effects. The offshore recording sites at Dunwich, Maplin and Holderness are in depths of 15m, 17.5m and 23m respectively but these are probably not truly in deep water and there may be wave refraction offshore of these depths. There are also offshore banks which could affect the waves. This leaves one remaining site, Perranporth. Of the 10 sites, this is the one which best fits the requirement of the PCM and NPM, that the coastline is approximately straight with parallel contours. At this site the seabed seems smooth and sandy so friction effects should be negligible. This site was chosen for calibrating the models. Further sites may be used in similar studies in the future.

2 DESCRIPTION OF THE COMPUTER MODELS

This chapter gives a description of the wave transformation computational models used in this study. The last section discusses the differences between the models.

All three models use as input incident wave conditions specified as directional spectra, $S(f,\Theta)$ (ie by functions describing the distribution of wave energy over both direction and frequency). The significant wave height (H_s) is the average height of the largest one third of the waves. The mean zero-upcrossing period (T_z) is the average time between successive upcrossings of the mean level by the water surface. The mean wave direction (Θ_w) is taken as the average of the spectral components over all frequencies and directions. They are approximated from the discretised spectrum by using the following equations:-

$$H_s = 4 \left(\sum_f \sum_\Theta S(f,\Theta)\right)^{1/2} ,$$

$$T_z = \left(\frac{\sum_f \sum_\Theta S(f,\Theta)}{\sum_f \left(\sum_\Theta S(f,\Theta) f^2\right)}\right)^{1/2}$$

and

$$\Theta_w = \Theta_o + \frac{\sum_f \sum_\Theta S(f,\Theta)(\Theta-\Theta_o)}{\sum_f \sum_\Theta S(f,\Theta)}$$

where Θ_o is the centre of the wave direction sector.

Each model produces corresponding frequency spectra (S(f)) at the inshore point of interest. The inshore H_s and T_z are calculated as above except there is no summation over θ.

2.1 The OUTRAY model

Twenty years ago, available modelling techniques consisted of little more than an estimation of refraction and shoaling effects by the hand-tracing of wave rays. These methods were time-consuming and error-prone and at best gave only a qualitative idea of refraction and shoaling. Modern methods rely on the use of computer models, which are both substantially quicker and more accurate than hand or graphical methods.

In the early 1970's, back-tracking ray models were developed in order to utilise the spectral representation of deep-water wave conditions and to reduce greatly the influence of caustics (where the rays converge) and dead areas (areas devoid of rays).

The back-tracking method is based on the principle of reversibility of ray paths, ie the path of a ray traced backwards (opposite to the actual direction of wave travel) is identical to the path traced forwards (in the direction of wave travel). The computational process involves tracing fans of rays at small angular increments from an inshore point of interest until they reach deep water. Some rays will not reach deep water and turn shorewards and strike the coast. These are ignored, and only rays reaching the offshore boundary are considered. The directions of these rays at the offshore boundary are grouped in angular 'boxes' (typically 10° wide) which represent a discretisation of the offshore directional spectrum. A discretisation of the period spectrum is obtained by

constructing a series of ray fans at regular period intervals.

The construction of these fans of rays allows the inshore spectrum to be determined in terms of the offshore spectrum. Refraction theory applied to wave spectra shows that the quantity $cc_g S(f,\Theta)$ is constant along a ray, where c is the wave celerity, c_g the group velocity, and $S(f,\Theta)$ the spectral function in frequency (f) and direction (Θ). The spectral function at an inshore point can then be determined in terms of the spectral function offshore as

$$S_i(f,\Theta) = \frac{c_o\, c_{g_o}}{c_i\, c_{g_i}} S_o(f,\Theta) \qquad (1)$$

where the subscript i denotes inshore values and o denotes offshore values. This method makes the assumption that $S_o(f,\Theta)$ is the same along the whole offshore boundary.

The OUTRAY back-tracking ray model is ideal for investigations where wave conditions are required at a small number of inshore points. Such applications would include evaluating wave conditions at entrances to harbours, at the locations of maritime works, or near beaches or dredged channels which are small in length.

The model has been used successfully at numerous sites both around the UK and in other parts of the world. It was specifically designed to represent the effects of depth refraction and shoaling and does not normally include the effects of currents and energy dissipation processes. In many cases this will not be a significant drawback and the model will give accurate

predictions of inshore wave conditions, even in very shallow water.

The Hydraulics Research method for calculating wave refraction as used in the OUTRAY model is described in Appendix 1.

2.2 The Parallel Contour Model (PCM)

The Parallel Contour Model is basically a simplified version of the OUTRAY model. The seabed is defined by supplying an offshore depth and the depth at the inshore point. The value of the direction of the beach normal is input and the contours are assumed to be normal to this.

Fans of rays and a set of transfer functions are constructed in the same way as in the OUTRAY model. Finding the ray paths is very simple because Snell's law can be used. This states that for waves progressively over a parallel contoured seabed

$$C/\sin \alpha = \text{constant}$$

where α is the angle between the wave crests and the contours and C is the wave celerity. From this we can obtain

$$\alpha_i = \sin^{-1} \left(\frac{C_o}{C_i} \sin \alpha_o\right)$$

where the subscripts o and i denote offshore and inshore. C_o and C_i can be calculated from the offshore and inshore depths for each frequency.

2.3 The Nearshore Profile Model (NPM)

The Nearshore Profile Model is a 1-D model which was developed for calculating wave, current and sediment transport parameters at a set of points on the shore-normal line. The grid points are not necessarily evenly spaced and are usually more concentrated close to the coast. The wave processes of shoaling, refraction (both by depth variations and currents), bottom friction, wave breaking, wave set-up and the generation of longshore currents are included. The model assumes a locally straight coastline with parallel depth contours. Tidal currents are generated by longshore variations in the water level (ie pressure-generated) with balancing forces supplied by bottom friction and inertia. Wave-induced currents are generated by spatial changes in the wave radiation stresses with, again, bottom friction and inertial balancing forces. The model is fully interactive in waves and currents, with waves influencing the currents through bottom friction and the generation of longshore currents, and currents influence the waves though bottom friction and refraction. Sediment transport rates are evaluated from the values of current velocity and seabed wave orbital velocity.

The theory is based on general mass, energy and momentum balance equations which are applicable both inside and outside the surf zone. The model can therefore be used for any profile length between offshore and the coastline, with no special treatment needed for the surf zone. The model can be used for any depth profile, and unlike some models is not restricted to monotonically decreasing depths.

The Nearshore Profile Model is of intermediate complexity between combined refraction/one-line beach

plan shape models and the 2-D and 3-D nearshore models. The model incorporates most of the physical processes that are found in 2-D nearshore models, but restricts its modelling to a single profile line assuming a straight beach with parallel depth contours. This reduction to 1-D greatly increases the computational efficiency, making the model capable of analysing the large number of input wave and tidal conditions (tens or hundreds of thousands of values) necessary for predicting long-term hydrodynamic and morphological processes. Despite the inclusion of many wave and current processes, and their interaction, the model is computationally very efficient.

Originally the NPM was restricted to regular waves only, but recently the model has been improved to cover the more realistic case of spectral waves. The theory of the spectral wave model is based on regarding the wave spectrum as composed of a number of individual frequency and directional components, each containing a certain amount of wave energy. The propagation of each component is considered independently of the other, except in the modelling of non-linear processes. In the present model the phenomena of refraction and shoaling (by both depth variations and currents) are treated linearly, while energy dissipation by bottom friction and wave breaking are non-linear processes. For the linear case, each directional component is represented by the central wave direction and the inshore wave direction is calculated using Snell's law. The offshore spectrum is then transformed into an inshore spectrum using equation (1).

More details about the NPM can be found in References 22,23 (monocromatic waves) and 24 (spectral waves).

2.4 Differences between the models

The three models each produce inshore wave conditions at one single inshore point but the NPM also gives results at each of the points at which the depths are given on the shore-normal. The OUTRAY model and PCM both produce a transfer function matrix which can be used to transform many wave conditions, whereas the NPM transforms each wave spectrum separately. The NPM includes seabed friction, wave breaking and tidal currents but these can be ignored if required. The other two models do not included non-linear effects or currents. The models each use a different representation of the seabed. OUTRAY uses a set of depth grids so the seabed can be described quite accurately. The PCM and NPM both assume parallel contours so they can only be used at sites where the coast is approximately straight and open to the sea, with very little variation in depth in the alongshore direction. They can cope with hollows and banks provided they stretch the length of the coast being modelled. The OUTRAY model and PCM use back-tracking ray projection methods. The NPM, however, can be regarded as being a forward-tracking method. Table 2 gives a summary of the differences between the models.

3 VALIDATION OF THE MODELS

3.1 Introduction

The site chosen for this study was Perranporth on the North Cornwall coast. The reasons for choosing this site was given in section 1.3. This chapter describes how the three models were used to transform offshore wave conditions into conditions at a point inshore for comparison with measured data at that point.

Three waverider buoys were situated off Perranporth (see Fig 1) and recorded over varying lengths of time from 1978 to 1981. There were two periods of simultaneous data. The offshore buoy (Site 2) was deployed by the Ministry of Defence, but HR obtained permission to record data from it for a previous study. It was about 11km offshore in a depth of about 48m at mid-tide. The inshore buoys were situated in 23m (Site 1) and 10m of water (Site 6). The 23m buoy was about 2km from the coast and was installed by HR. The position of this buoy is regarded as "inshore" because there is likely to be wave refraction offshore of this position, especially for waves with long wave periods which can occur from the south west, from the Atlantic. The 10m buoy was installed by HR for a project sponsored by MAFF. The first period of wave recordings was 10 months long over the winter of 1978/79 at Sites 1 and 2. The second period was for 15 months starting in September 1980 at Sites 1 and 6.

The second period of wave recording at the two inshore sites was not used in the calibration because the wave transformation models require offshore wave conditions as input. It would have been possible to use this period by predicting the offshore wave conditions, refracting them to the 23m buoy, and then refracting them on to the 10m buoy. But this would have been much more difficult than using the first period of field data and there would be much dependence on the offshore wave predictions.

Reference 17 describes the analysis of the raw wave data and a statistical analysis of the wave parameters. In that report only the results from the counting analysis method for analysing raw wave data were used. For this study the results from the spectral analysis have been used since the models to

be calibrated each use spectral input. This method of analysis is described in Reference 25.

A refraction study at Perranporth was carried out at HR in 1982 (Ref 18) but only comparisons with the wave data as a whole were carried out rather than for individual storms. Often when predicting wave conditions it is the highest waves and extremes which are required rather than waves only 1 or 2m high. Therefore this calibration study has concentrated on the higher waves.

The next section describes how the storms were chosen for use in the calibration. Section 3.3 describes how the measured offshore frequency spectra were converted into directional spectra. The setting up and running of the models is described in section 3.4. To test the sensitivity of the models to the offshore wind direction a hypothetical storm was input to the models from numerous directions and the results of this test are given in section 3.5. The model results for the chosen storms are discussed in the final section.

3.2 Choice of storms

The period of simultaneous wave recording at the offshore and inshore sites was 30th August 1978 to 27th June 1979. The offshore buoy (Site 2) was about 11km offshore in a depth of about 48m at mid-tide. The inshore buoy (Site 1) was about 2km from the coast and in a depth of about 23m.

Twenty to thirty offshore storms were required for calibrating the wave transformation models. The storms with the highest wave heights were chosen because there is likely to be more refraction for these than for the smaller waves. Wave records with wave heights above 3m were chosen. A few of these

storms occurred when the wind direction was not towards the coast and the inshore buoy. The models only take into account waves that are refracted in from offshore. Locally generated waves travelling away from the coast are not modelled, so these storms were not used in this calibration exercise.

A list of the offshore storms chosen is given in Table 3 along with the corresponding inshore conditions and the ratio of inshore to offshore wave height and wave period. One of the storm wave heights is 10% higher at the inshore buoy than offshore. The inshore wave height was recorded 14 minutes after the offshore wave height was recorded. The wave probably took over 30 minutes to travel between the two buoys. Therefore, the inshore wave height corresponding to the offshore wave height should probably be lower than quoted in Table 3. The increase in wave height from offshore to inshore could be due to local focussing of the waves and shoaling. The highest wave height was just over 7m offshore and this decreased by 18% by the time it reached the inshore site.

3.3 Creation of the offshore directional spectra

The wave transformation models require as input homogeneous directional wave spectra. The frequency spectrum for each storm was obtained from the spectral analysis of the field wave data, but the wave riders did not record any form of direction. It was therefore necessary to augment the measurements with a directional spread derived by mathematical modelling.

Wind-generated waves usually show some directional spreading about their mean direction of propagation. Wind travelling over a water surface transmits energy to the water in directions on either side of its own

direction. In order to convert the frequency spectra into directional spectra, the mean wave direction is required for each storm together with the directional spread about this mean.

A wave prediction model was used to obtain the wave directions. This model is called HINDWAVE and it predicts wave conditions using winds recorded at a nearby anemometer station. It is described in Appendix 2.

The position of the offshore buoy was taken as the wave prediction point. Wind records were obtained from the Meteorological Office for the required period (September 1978 to June 1979). They were recorded at St Mawgan which is about 15km north east of Perranporth. The anemometer is about 2½km inland. Winds blowing over the sea are usually higher than those blowing over the land because there is less friction. A study in the Severn Estuary (Ref 26) showed that the wind speeds at St Mawgan should be multiplied by 1.3 to get the equivalent wind speed over water. The same wind speed-up factor was used for this study.

The JONSWAP/SEYMOUR wave prediction model is a sub-model of HINDWAVE and it is also described in Appendix 2. This model was initially run using the standard value for the peak enhancement factor, $\gamma = 3.3$ (also described in Appendix 2). Comparing the predicted wave spectra with the measured showed that the peak of the spectra and the significant wave height for the predicted storms were too high, indicating that this factor should be reduced. A value of $\gamma = 1$ was then used. This reduces the JONSWAP spectrum to the Pierson-Moskowitz spectrum for a fully developed sea, except that α and f_m are

dependent on the fetch length. This gave better results. Many of the measured spectra contained high energies in the low frequencies which were not predicted by the HINDWAVE model and these were probably produced by swell. To incorporate this swell into each direction spectrum the directional spread about the mean wave direction for the predicted spectrum was applied to the measured spectrum. Figure 2 shows the frequency spectrum for storm 4 and Figure 3 shows corresponding directional wave spectrum.

To create these spectra, 36 wave direction bands with a width of 10° and 15 wave period bands were used. For most of the storms periods from 3 to 17 seconds in steps of 1 second were used. For the 2 storms with the highest values of T_z (storms 8 and 9) higher periods were necessary, and so 4 to 32 seconds in 2 second steps were used.

3.4 Setting up and running of the models

This section describes how the wave transformation models were set up to transform the offshore directional wave spectra into wave conditions at the site of the inshore waverider buoy (Site 1). The results are discussed in Sections 3.5 and 3.6.

A previous study at Perranporth (Ref 18) had shown that the effect of the tidal range is small, so only one tidal level, Mean Sea Level (0.25m above ODN) was used in all the models for this study.

3.4.1 The OUTRAY model

The first step in using the OUTRAY model is to represent the seabed over the area of interest using a

set of grids of depth values. Each grid is rectangular and sub-divided into smaller rectangles. A depth value is read off the chart at each corner of these smaller rectangles. A suitable grid already existed which had been used in the earlier study at Perranporth. The grid system is shown in Figure 4. It extends over 20km either side of Perranporth to ensure that all incoming waves of importance are correctly modelled. The offshore boundary lies in a water depth of about -50m ODN. The system consists of 6 grids with the x-axis making an angle of 36.5 degrees with north. Details of the grid system are given in the table below.

Perranporth Refraction Grid System

Grid number	Internal Spacing (m) x	y	Number of grid lines columns	rows
1	600	600	73	11
2	600	600	14	9
3	600	600	11	11
4	400	400	26	17
5	400	400	16	16
6	600	600	21	9

In this table columns are lines parallel to the y-axis and rows are lines parallel to the x-axis. The inshore point (Site 1) was situated in grid 4.

For each frequency an inshore angular ray separation was selected. Since the shorter period waves do not 'feel' the sea bed in deeper water it is possible to use larger separations for these waves. On the other hand since longer period waves refract more, a smaller angular separation is required to give an accurate picture of their refraction behaviour. The angular separations which were used are 1° upto 7s, 0.5° between 8 and 11s and 0.25° for periods above 12.

A transfer function was then evaluated using the same periods and wave directions are for the offshore directional wave spectra. This was used to convert the 26 offshore spectra into equivalent conditions at the inshore waverider site.

3.4.2 The Parallel Contour Model (PCM)

In this model the seabed is represented by inputting the total depth on the offshore boundary, the depth at the inshore point and the direction of the beach normal. For Perranporth, these values were 48.25m, 23.25m and 285°N respectively. The beach normal is shown on Figure 4. A test was carried out to see how dependent the model was on the accuracy of the measurement of the beach normal by using a value of 300°N. The results of this test are described in Section 3.5.

A transfer function was created and used to transfer the offshore waves to inshore as in the OUTRAY model.

In this model the waves are allowed to reach the inshore point from 90 degrees either side of the beach normal. To the south west of Perranporth is St Agnes Head and the western tip of Cornwall which may stop waves from the south south west from reaching Perranporth. To the north north east there is Penhale Point which may stop waves from this direction too. Another two transfer functions were created with wave directions restricted to 235-15°N (clockwise) instead of 195-15°N for a shore normal of 285° and 210-30°N for a shore normal of 300°N. The results from using the transfer functions are compared in the next chapter.

3.4.3 The Nearshore Profile Model (NPM)

In the NPM the seabed is represented by inputting depth values at points along the beach normal. The beach normal was taken as 285° as in the PCM and the depth profile used is shown in Figure 5. Calculations were carried out ignoring breaking and friction for comparison with OUTRAY and PCM. Further calculations were carried out using both seabed friction and wave breaking separately. Tests were also carried out using a beach normal of 300° and restrictions on the wave direction as in the PCM. The results are given in the next two sections.

3.5 Results for a hypothetical storm

A test was carried out to see how sensitive the models are to the offshore wave direction. An offshore directional spectrum was created using a single fetch length of 100km for all wave directions. The wave height was 3.5m and the wave period was 6.5s. This storm was input to the wave transformation models using mean wave directions from 200° to 40°N (clockwise) in 10° increments.

Figure 6 shows the curve of the offshore to inshore wave height ratio against the offshore wave direction for the OUTRAY model. It can be seen that the OUTRAY model gives the least reduction in wave height from offshore to inshore for an offshore wave direction of 300°N. Figure 7 shows the curve of the inshore against offshore wave direction. For an offshore wave direction of 300°N, the inshore wave direction from OUTRAY is also 300°N. Waves from other directions bend towards 300°N as they travel inshore. This implies that the normal to the beach in the OUTRAY model is approximately 300°N, not 285°N as measured

for the other two models. Figures 6 and 7 also show the results from the PCM for beach normals of 285 and 300°N allowing the waves to reach the inshore point up to 90° either side of the normal. For the PCM, the highest inshore wave height occurs when the offshore wave direction is along the beach normal. Altering the beach normal by 15° from 285 to 300°N moves the wave height ratio curve right 15°. The curve is symmetrical about the beach normal because the model assumes the seabed is symmetrical about this line. The wave direction curve has rotational symmetry about the beach normal. Increasing the beach normal by 15° moves the curve up 15° and right 15°.

The maximum wave heights given by OUTRAY and the NPM are about the same but the wave height decreases more rapidly in the OUTRAY model as the offshore wave direction moves away from the normal. For waves from south west to west the wave direction has altered less for the PCM than OUTRAY as the waves travel inshore. From the North the wave directions from OUTRAY lie between those from the two sets of PCM results. The main reason for the difference between results from the two models is that the PCM assumes the coast is straight while OUTRAY models the curvature of the contours at either end of Perran Bay. To represent the sheltering from St Agnes Head and Penhale Point at either end of the Bay in the PCM, waves were only allowed to reach the inshore point from 235 to 15°N. The results from these further tests are shown in Figures 8 and 9. With these restrictions on the wave direction the results from the PCM are very similar to the OUTRAY model for these hypothical storms, especially when a beach normal of 300°N is used.

Figures 10 and 11 show the results from the NPM allowing waves from 90° either side of the beach normal. The results are almost identical to those

from the PCM. The tests were rerun using the restriction on inshore wave direction as used for the PCM. These results are shown in Figures 12 and 13. Again these are similar to the results from the PCM. Waves from the south west are slightly higher and waves from the north are lower than those from the PCM. This is mainly because in the NPM the only way to restrict the wave directions is to set the values in the direction bands in the spectra to zero. These bands are 10° wide starting at 0°N, therefore 235-15°N had to be replaced with 240-10°N.

The NPM was rerun with wave breaking included. The results were identical to those which were calculated without wave breaking. This implies that the wave heights are not high enough, in this depth of water, for wave breaking to occur. However higher wave heights might break, so it can not be ignored completely. The model was also rerun with the effects of seabed friction included. The wave heights were less than 0.5% smaller than those excluding the effects of seabed friction. For these wave heights the friction effect is small but it may be significant for higher wave heights.

3.6 Results for the storms

This section describes the results from transforming the 26 offshore wave spectra into conditions at the inshore point using all three models. The results are compared with the measured data.

Figure 14 shows the inshore to offshore wave height ratio for the results from OUTRAY against the wind direction. The reduction in wave height appears to be very dependent on wind direction. Nearly all the points lie on a curve except for the two highest wave heights which are probable affected by swell.

Figure 15 shows the equivalent graph from the measured data. The points are much more scattered. For example, the two storms with wind directions of 15°N (385°N) have similar wave heights but one is reduced by 37% while the other is only reduced by 17%. The curve shown on the figure is the best fit curve for the OUTRAY results (ie the points shown in Fig 14). It can be seen that this is very similar to the best fit curve of the measured data. The measured data is recorded at 3 hourly intervals. The waves might take about 30 minutes to travel from the offshore point to inshore. Therefore the inshore wave height may have changed since the recording time and the measured ratios may not be correct. This may be one reason for the scatter of the measured data. Results from the PCM and NPM show a similar dependence on offshore wind direction.

Table 4 shows the percentage over-prediction of the wave heights for the four runs of the Parallel Contour Model. These runs were for beach normals of 285 and 300°N, with and without the restriction on the inshore wave angle. In general the best results were obtained for a beach normal of 300°N and wave directions restricted to 235-15°N. The original beach normal measured from the charts was 285°N which would predict wave heights on average 2% higher than using a beach normal of 300°N.

Table 5 shows the percentage over-prediction of the wave heights for the four runs of the Nearshore Profile Model ignoring the effects of friction. As for the PCM the best results in general are obtained using a beach normal of 300°N and restricting the waves to 235-15°N. Table 6 shows the results including the effects of friction. The seabed friction decreases the wave heights by about 1 or 2%. The two storms with wind directions at 90° to the

beach normal of 285°N (storms 11 and 13) are under-predicted by over 50% when friction is taken into account. The model is probably not valid for such oblique angles and the average overprediction of 2.8% is lower than it should be because of the inclusion of these 2 storms. The friction factor used in the model was 0.016 but this was arbitary because the amount of seabed friction is not known at this site. This is the factor most commonly used when friction is known to occur. Increasing this factor will reduce the wave heights even more. Results including wave breaking were identical to those ignoring it.

A comparison of the results of the three models is given in Table 7. The beach normal used in the PCM and NPM was 300°N with wave directions restricted to 235-15°N. On average the best results were obtained from the OUTRAY model which has the most accurate representation of the seabed of the three models. The average percentage overprediction was 1.7% for OUTRAY. Assuming a Gaussian probability distribution, there is a 95% chance that the overprediction will be in the range -19.2 to 22.6%. For the PCM the average overprediction was 6% with a 95% chance of it being in the range -14.8 to 26.8%. The NPM without seabed friction and wave breaking effects also had an average of 6%. Since the NPM and PCM both represent the seabed in the same way they would be expected to give similar results. The differences of 1 to 2% occurred because the NPM used one ray for each offshore direction box, ie at 10° intervals, but the PCM used ray separations of 0.25 to 1° at the inshore point, depending on the wave period. So the PCM would have been more accurate. The results of the Nearshore Profile Model were improved by including the effects of seabed friction but most of the storm wave heights were still over-predicted by more than those from the

OUTRAY model. The percentage reduction in wave height due to seabed friction can be taken from the results of the NPM and applied to the OUTRAY wave heights. This reduces the OUTRAY wave height by between 0.5 and 4.1%. For example storm 8 (the highest wave height) would only be over-predicted by 5.5% instead of 9.6%, storm 5 by 11.9% and storm 23 by 15.6%, assuming that a friction factor of 0.016 is correct.

The mean inshore wave directions calculated by the models are given in Table 8. The wave direction was not recorded at the inshore site so no comparisons can be done with measured data. The predicted inshore wave directions from the PCM and NPM are within 2° of each other. Directions from OUTRAY and the PCM are within 5° of each other. The greatest difference in direction is mainly when the wind direction is far from the beach normal.

4 DISCUSSION

The site chosen for this calibration study has an approximately straight coastline with parallel seabed contours. It faces open sea and the seabed is fairly smooth and even. All of the above are required so that the PCM can be used. The PCM requires the depths to be monotonically decreasing towards the shore but the NPM will allow trenches and banks on the seabed provided they stretch the length of the coast. The OUTRAY model can use nearly any sort of seabed provided the depths only vary gently. The OUTRAY model and PCM do not include wave breaking or tidal currents so they would not be applicable where these occur. Also they do not include seabed friction but the reduction in wave height due to friction could be calculated by another model and then be applied to the results. The NPM can include the effects of wave breaking, friction and currents.

The PCM and NPM have the orientation of the beach defined by inputting the value of the beach normal. The beach normal measured off the charts for Perranporth was 285°N. A trial run of the OUTRAY model using a hypothetical storm from various directions showed that a beach normal of 300°N was probably more realistic. The models were run using both 285 and 300°N as the beach normal. A beach normal of 300°N gave the best results. If a run of the OUTRAY model had not been carried out before hand, the beach normal of 285°N would have been assumed to be correct, giving poor results. The beach normal was measured from a chart which probably had insufficient depth data to obtain a correct alignment of the contours. The coast at Perranporth is not completely straight because it is a large bay, Perran Bay. To take this into account in the models the wave energy was restricted to directions from 235 to 15°N. For other sites it is possible that similar restrictions could be used. Waves travelling near to the bounds of the restriction may not be modelled very well but should be better than without the restriction.

5 SUMMARY AND CONCLUSIONS

This report has considered the transformation of wave energy from offshore to an inshore site using some of HR's wave transformation models. The models were calibrated using field wave data. A literature review was carried out and a site with suitable data was chosen. This site was Perranporth. Three computational models were chosen for the calibration exercise. They were the OUTRAY back-tracking ray model, the Parallel Contour Model (PCM) which is a simplified version of OUTRAY, and the Nearshore Profile Model. 26 storms were chosen from the wave recording period between August 1978 and June 1979. Directional wave spectra were created for these storms

using the measured frequency spectra and the predicted wave direction and directional spread about this direction. The spectra were then transformed into inshore wave conditions using each of the models.

The 26 chosen storms had offshore wave heights over 3m with the maximum wave height being 7.05m. The offshore wave periods ranged from 6.1 to 10.6 seconds and the directions ranged from 227 to 25°N. On average the inshore predicted wave heights exceeded the measured by 1.7% from OUTRAY, 6% from the PCM and NPM without friction effects and 4.7% from the NPM including friction effects. The corresponding over-prediction of inshore wave period was 2.7%, 5.7%, 8.7% and 8% respectively. The results from all three models were much more dependent on the wave direction than the measured data.

The results of the Nearshore Profile Model showed that wave breaking is negligible at the inshore position. It is situated in 23m of water so it was unlikely that there would be wave breaking. The OUTRAY model gave the results closest to the measured data. This is the most complex of the models and has the most accurate representation of the seabed. The PCM and NPM results are dependent on the accuracy of the beach normal which is supplied to the models. At Perranporth the beach normal measured from the chart appears to be 15° out from the true normal. A more detailed chart may have given a better approximation for the alignment of the contours.

The NPM indicated that seabed friction had some effect on the wave heights, probably reducing them by 1 or 2%.

Of the three models OUTRAY is probably the best one to use for such a study provided the depth data is

available and there is enough time and money. The PCM should only be used when the results do not have to be accurate or not enough is known about the seabed topography and an approximation would do. If only wave refraction and shoaling is required the OUTRAY model is preferable from the NPM. However the NPM can include seabed friction, wave breaking and current interaction which are excluded from the other two models. It also calculates values at points along the shore normal.

It is recommended that more of HR's wave refraction models are validated against field wave data. HR's finite difference model including frictional effects could be calibrated against the storms used in this study. The models verified in this study could also be used along with other models for Holderness. The HR HINDWAVE model could be used to hindcast waves at Flamborough, at the site of a waverider. These predictions could then be calibrated against the field data at Flamborough which would include wave directions because it was measured by a WAVEC waverider. Then this offshore data could be refracted inshore to the Holderness inshore buoy for comparison with the field data there. Model calibrations could also be carried out at sites where tidal currents are likely to affect the waves. A version of OUTRAY has been developed which includes current-depth refraction of waves and this model will be calibrated with field data at Shakespeare Cliff during 1989-90.

6 ACKNOWLEDGEMENTS

This study was carried out by Miss C E Jelliman and was supervised by Dr A H Brampton. They are members of the Coastal Processes Section, within the Maritime Engineering Department, headed by Dr S W Huntington. The author would like to thank her colleagues

Dr P J Hawkes and Mr H N Southgate for advice during this study.

7 REFERENCES

1. Aberdeen Harbour - Report on Phase II studies. HR Report EX 1759, July 1988.

2. Aldeburgh sea defences. HR Report EX 1465, July 1986, confidential to C H Dobbie and Partners and Anglian Water.

3. Hawkes P J. A wave hindcasting model. Modelling the Offshore Environment, Society for Underwater Technology, April 1987.

4. Wave recording at Barrow in Furness - 1987-88. HR Report EX 1840, January 1989.

5. Cardiff Bay Barrage Feasibility study. Re-calibration of wave prediction/refraction models. HR Report EX 1857, January 1989.

6. Validation of wave direction predictions at Shakespeare Cliff - preliminary report. HR Report EX 1855, February 1989.

7. Hengistbury Head coast protection study. Technical Report. HR Report EX 1460, July 1986.

8. Wave study for the Arun coast. HR Report EX 1871, March 1989.

9. Pittenween Harbour, Fife, Scotland. Wave measurements and calibration of mathematical models. HR Report EX 1611, November 1987.

10. Swanage Yatch Habour. Further Wave and Littoral Drift study. HR Report EX 1573, April 1987.

11. Sea defence management study for the Anglian region. Offshore wave climate. HR Report EX 1665, January 1988.

12. Tucker M J, Carr A P and Pitt E G. The effect of an offshore bank in attenuating waves, Coastal Engineering, Vol 7, ppl33-144, 1983.

13. Falmouth container terminal. Wave analysis offshore and at the proposed site. HR Report EX 1365, March 1986.

14. The MIAS catalogue of instrumentally measured wave data, 1984.

15. Shoeburyness sea defences - studies of wave conditions and seawall performance. HR Report EX 1641, October 1987, confidential to the Property Services Agency (Eastern Region).

16. The Wave Climate at Maplin - A field wave recording exercise. HR Report EX 655, September 1974.

17. Bellamy P H. Statistics of waves recorded off the North Cornwall Coast, HR Report IT 235, August 1982.

18. Study of wave spectra transformation. HR Report EX 1063, June 1982.

19. Dingemans M W, Stive M J F, Kuik A , Radder A C and Booij N. Field and laboratory verification of the wave propagation model CREDIZ, Proc. 19th Int. Conf. on Coastal Eng., Houston, 1984.

20. Wang H and Yang W-C. Wave spectral transformation measurements at Sylt, North Sea, Coastal Engineering, Vol 5, pp1-34, 1981.

21. Wave data around the coast of England and Wales - A Review of Instrumentally Recorded Information. HR Report SR 113, February 1987.

22. Southgate H N. A one-dimensional model of wave-current interaction, ASCE Speciality Conference on Coastal Hydroydnamics, Delaware, USA, 1987.

23. Southgate H N, The nearshore profile model, Report SR 157, Hydraulics Research Ltd, February 1988.

24. Southgate H N, The nearshore profile model incorporating wave spectra, Report SR 201, Hydraulics Research Ltd, March 1989.

25. Brampton A H. A computer method for analysing wave records, HR Report IT 301, October 1985.

26. Severn Tidal Power - Hindcasting Extreme Waves, HR Report EX 978, March 1981.

TABLES.

TABLE 1 List of data sources for validation

Sites with inshore field data only

Location	Models used in previous studies	References (see Reference section for more details)
Aberdeen	O/N	EX 1759 (Ref 1)
Aldeburgh	O	EX 1465 (Ref 2) and SUT (Ref 3)
Barrow	O	EX 1840 (Ref 4)
Cardiff	O	EX 1857 (Ref 5)
Folkestone	O	EX 1855 (Ref 6)
Hengistbury Head	O	EX 1460 (Ref 7)
Littlehampton	O	EX 1871 (Ref 8)
Pittenween	O	EX 1611 (Ref 9)
Swanage	O	EX 1573 (Ref 10)

O - Combined OUTRAY and HINDWAVE

N - Nearshore Profile Model

(Cont'd)

TABLE 1 (Continued)

Sites with both simultaneous offshore and inshore field data

Location	Models used in previous studies	Models that could be used	Comments and References
Dunwich	H	O/N/P	EX 1665 (Ref 11) describes an offshore wave prediction which was calibrated against field data. Tucker (Ref 12) investigated wave transmission over Dunwich Bank using data from November 78 to May 79. There were four sites. A waverider measured waves offshore in a depth of 15m from August 77 to May 79. Inshore there was one pressure sensor in 8m of water (15.4.75-Mar 79) and two waveriders in 5.5m (28.8.75-12.6.76) and 8m (Nov 78 - May 79). HR holds but does not own part of the data from the pressure sensor.
Falmouth		O	EX 1365 (Ref 13) describes the analysis of the field data at both the offshore and inshore locations. The coast is not straight enough and the bed topography is too complicated for the models which assume parallel contours. Seabed friction may be important. HR holds but does not own the data. A waverider recorded offshore in a depth of 45m from 6/6/84-31/5/85 and a pressure sensor recorder inshore in a depth of 7m from 5/6/84-21/3/85.
Great Yarmouth		O/N/P	Waverider buoys recorded data in depths of 25m (14.12.84-11.12.85) and 12m (14.12.84-9.12.85). HR holds but does not own the data.

(Cont'd)

TABLE 1 (Continued)

Sites with both simultaneous offshore and inshore field data

Location	Models used in previous studies	Models that could be used	Comments and References
Holderness	H	O/N/P	EX 1665 (Ref 11) describes an offshore wave prediction calibrated against field data. Waverider buoys recorded in 23m (Apr 86-Mar 86) and 19m of water (Apr 86-Jun 86). HR holds but does not own the data.
Lowestoft		O/N/P	MIAS Catalogue (Ref 14). Waveriders recorded in 40m (Dec 75-Feb 77) and 5.6m of water (22.7.74-25.9.79). Date quality and availability not known.
Maplin	H	O/N/P	EX 1641 (Ref 15) describes an offshore wave prediction calibrated against field data. EX 655 (Ref 16) describes the wave recording at one offshore and five inshore sites. The offshore waverider was in a depth of 17.5m (1.4.73-31.3.75) and the inshore waveriders were in a depth of 8.5m (Early 73-Mid 74). HR holds the data but does not own it.
Perranporth		O/N/P	IT 235 (Ref 17) describes the wave recording at 3 sites. EX 1063 (Ref 18) describes a wave refraction study (OUTRAY) but no storm comparisons were carried out. Waveriders recorded in depths of 45m (30/8/78-27/6/79), 23m (26/9/80- 14/12/81) and 8.5m of water (13/11/75-2/3/86). HR owns the data.

(Cont'd)

TABLE 1 (Continued)

Sites with both simultaneous offshore and inshore field data

Location	Models used in previous studies	Models that could be used	Comments and References
South Uist (Outer Hebrides)		O/N/P	EX 1063 (Ref 18) describes two wave refraction studies (OUTRAY and a finite difference model) but no storm comparisons were carried out. Conclusions were that non-linear effects could not be ignored. The waveriders were situated in depths of 44m and 23m.
Haringvliet (Holland)		O/N/P	Dingemans (Ref 19) describes a comparison of a parabolic model with field data. 7 recording sites, the offshore waverider recorded wave direction.
Sylt (N Germany)		O/N/P	Wang and Yang (Ref 20) describes a wave refraction exercise.

O - OUTRAY
N - Nearshore Profile Model
P - Parallel Contour Model (Simple Snell's law)
H - Hindwave used to create offshore climate which was calibrated using the offshore field data.

TABLE 2 Difference between OUTRAY, PCM and NPM

Model	OUTRAY	PCM	NPM
Representation of seabed	depth grids input	parallel contours with only inshore and offshore depths input	parallel contours with depths input at points along the shore normal
Type of Bathymetry	Reasonably gentle depth variations	very little depth variation in the alongshore direction	very little depth variation in the alongshore direction but depths need not be monotonically increasing to offshore
Type of Coastline	any, except, where external diffraction is important (eg shelter by a headland)	approximately straight coast facing open sea	approximately straight coast facing open sea
<u>Wave Processes Incorporated</u>			
Depth Refraction and Shoaling	Yes	Yes	Yes
Current Refraction	No	No	Yes
Bottom Friction	No	No	Yes
Wave Breaking	No	No	Yes

TABLE 3 Storm conditions used in the models

Recorded by waverider buoy at Perranporth

Storm No.	yr	day	mon	Offshore (site 2) time (min)	Hs_o (m)	Tz_o (s)	Inshore (site 1) time (min)	Hs_i (m)	Tz_i (s)	Hs_i/Hs_o	Tz_i/Tz_o	Predicted Wind Direction (°N)
1	78	9	11	726	3.956	7.00	731	3.460	6.72	0.875	0.960	248
2	78	9	27	536	3.159	6.26	523	2.986	6.22	0.945	0.994	287
3	78	9	29	733	4.657	7.10	713	4.261	7.13	0.915	1.004	295
4	78	10	17	1089	3.697	6.30	1086	3.209	6.24	0.868	0.990	308
5	78	11	15	1438	4.403	7.64	1269	3.534	6.60	0.803	0.864	275
6	78	11	21	1076	3.162	7.28	1081	3.034	7.05	0.960	0.968	227
7	78	11	25	1430	3.434	6.18	160*	3.327	6.21	0.969	1.005	317
8	78	12	12	1435	7.053	10.52	1435	5.798	9.58	0.822	0.911	229
9	78	12	14	168	5.978	8.49	178	5.483	8.57	0.917	1.009	243
10	79	1	10	1424	5.173	7.39	1418	4.549	7.36	0.879	0.996	302
11	79	1	17	1073	3.180	6.05	1062	2.016	5.98	0.634	0.988	25
12	79	1	30	160	3.334	6.08	162	2.805	6.21	0.841	1.021	265
13	79	3	15	1261	3.209	6.34	1262	2.652	6.47	0.826	1.021	25
14	79	3	3	730	3.371	8.03	723	2.955	7.20	0.877	0.897	235
15	79	3	7	730	4.237	7.31	723	3.553	6.55	0.839	0.896	275
16	79	3	9	539	4.390	7.51	534	3.491	6.83	0.795	0.909	241
17	79	3	10	1439	3.169	6.60	1*	2.756	6.14	0.870	0.930	263
18	79	3	11	730	3.276	6.54	724	2.938	6.68	0.897	1.021	243
19	79	3	26	171	4.799	7.27	185	5.268	7.65	1.098	1.052	263
20	79	3	28	371	4.493	7.22	367	4.060	6.95	0.904	0.963	279
21	79	3	29	177	5.848	7.67	191	4.802	7.34	0.821	0.957	351
22	79	4	23	1271	3.556	6.69	1274	3.165	6.56	0.890	0.981	282
23	79	4	24	546	4.461	7.52	541	3.383	6.52	0.758	0.867	337
24	79	5	1	905	3.159	6.12	917	3.179	6.06	1.006	0.990	318
25	79	5	17	549	4.124	7.53	544	3.385	6.98	0.821	0.927	240
26	79	6	15	188	3.372	6.16	202	2.332	5.49	0.692	0.891	285

* next day

TABLE 4 **Results from the Parallel** Contour Model

Percentage overprediction of wave height

Storm No.	Wind Direction (°N)	Model Run No. * 285	285a	300	300a
1	248	9.8	7.9	6.5	5.1
2	287	1.2	0.6	0.0	-0.4
3	295	5.6	5.4	4.4	4.3
4	308	9.4	9.3	9.6	9.3
5	275	21.5	20.8	18.9	18.2
6	227	-0.1	-3.0	-4.8	-7.0
7	317	-2.4	-2.4	-1.4	-2.0
8	229	20.8	21.7	13.1	13.6
9	243	4.5	5.8	0.3	1.0
10	302	10.2	10.1	10.1	9.9
11	385	-4.6	-4.6	17.4	7.6
12	265	13.6	11.9	11.7	10.2
13	385	-26.3	-26.3	-9.2	-14.9
14	235	10.4	8.1	5.0	3.3
15	275	16.3	15.5	13.7	13.1
16	241	19.1	16.9	14.7	13.0
17	263	10.3	9.0	7.6	6.4
18	243	7.7	5.0	4.3	2.2
19	263	-12.5	-13.3	-14.8	-15.6
20	279	5.8	5.3	3.7	3.2
21	351	-4.3	-4.3	5.6	4.1
22	282	9.0	8.3	7.3	6.9
23	337	18.1	18.1	24.1	22.8
24	318	-6.4	-6.4	-5.5	-5.9
25	240	17.4	14.9	12.5	10.6
26	285	38.0	37.1	36.6	36.0
Average Percentage Overprediction		7.4	6.6	7.4	6.0

* Definition of model runs

285 - Beach normal 285°N. Rays allowed 195-15°N
285a - Beach normal 285°N. Rays allowed 235-15°N
300 - Beach normal 300°N. Rays allowed 210-30°N
300a - Beach normal 300°N. Rays allowed 235-15°N

TABLE 5 Results from Nearshore Profile Model - without friction

Percentage overprediction of wave height

Storm No.	Wind Direction (°N)	Model Run No. * 285	285a	300	300a
1	248	9.7	8.9	6.4	5.7
2	287	1.8	1.8	0.7	0.6
3	295	5.4	5.4	4.2	4.2
4	308	9.7	9.7	9.8	9.6
5	275	21.6	21.2	18.9	18.6
6	227	-0.1	-1.7	-4.7	-5.9
7	317	-2.2	-2.3	-1.4	-1.8
8	229	23.1	22.0	14.8	14.0
9	243	7.3	6.6	2.4	1.8
10	302	9.7	9.7	9.6	9.5
11	385	-5.2	-5.5	19.0	2.3
12	265	14.1	13.7	12.2	11.8
13	385	-26.8	-27.1	-8.5	-19.2
14	235	10.4	9.0	5.2	4.1
15	275	15.8	15.5	13.2	12.9
16	241	19.6	18.3	15.2	14.2
17	263	11.1	10.6	8.3	7.9
18	243	7.1	5.9	3.8	2.7
19	263	-12.5	-12.8	-14.9	-15.2
20	279	5.9	5.8	3.8	3.7
21	351	-3.8	-3.9	6.5	2.6
22	282	8.3	8.2	6.7	6.6
23	337	18.1	18.0	24.3	22.1
24	318	-6.2	-6.2	-5.3	-5.8
25	240	17.4	16.0	12.6	11.4
26	285	38.0	38.0	36.7	36.6
Average Percentage Overprediction		7.6	7.1	7.7	6.0

* Definition of model runs

285 - Beach normal 285°N. Rays allowed 195-15°N
285a - Beach normal 285°N. Rays allowed 235-15°N
300 - Beach normal 300°N. Rays allowed 210-30°N
300a - Beach normal 300°N. Rays allowed 235-15°N

TABLE 6 Results from Nearshore Profile Model - with friction

Percentage overprediction of wave height

Storm No.	Wind Direction (°N)	Model Run No. * 285	285a	300	300a
1	248	8.5	7.8	5.1	4.5
2	287	1.2	1.1	0.1	0.0
3	295	4.3	4.3	3.1	3.1
4	308	9.1	9.0	9.2	9.0
5	275	19.9	19.5	17.2	16.8
6	227	-1.4	-3.0	-6.1	-7.4
7	317	-2.8	-2.8	-1.8	-2.3
8	229	19.2	18.2	10.7	9.9
9	243	5.2	4.4	0.1	-0.5
10	302	8.4	8.4	8.3	8.2
11	385	-57.9	-6.0	18.2	1.6
12	265	13.4	13.0	11.4	11.0
13	385	-68.8	-27.9	-9.5	-20.1
14	235	8.6	7.3	3.3	2.2
15	275	14.4	14.1	11.8	11.5
16	241	18.1	16.8	13.5	12.4
17	263	10.0	9.5	7.2	6.7
18	243	6.1	4.9	2.7	1.6
19	263	-13.6	-13.9	-16.1	-16.4
20	279	4.8	4.7	2.6	2.5
21	351	-5.4	-5.5	4.9	1.1
22	282	7.5	7.4	5.8	5.7
23	337	16.5	16.5	22.8	20.7
24	318	-6.8	-6.8	-5.8	-6.3
25	240	15.7	14.2	10.8	9.6
26	285	37.4	37.2	35.9	35.9
Average Percentage Overprediction		2.8	5.9	6.4	4.7

* Definition of model runs

285 - Beach normal 285°N. Rays allowed 195-15°N
285a - Beach normal 285°N. Rays allowed 235-15°N
300 - Beach normal 300°N. Rays allowed 210-30°N
300a - Beach normal 300°N. Rays allowed 235-15°N

TABLE 7 Results from all 3 models

Storm No.	Wind Direction (°N)	Percentage over-prediction of inshore H_s				Percentage over-prediction of inshore T_z			
		OUTRAY	PCM	NPM (no friction)	NPM (friction)	OUTRAY	PCM	NPM (no friction)	NPM (friction)
1	248	-0.3	5.1	5.7	4.5	3.1	5.3	8.2	7.6
2	287	-2.6	-0.4	0.6	0.0	-1.7	-0.6	4.5	4.2
3	295	1.3	4.3	4.2	3.1	-2.4	-1.2	1.8	1.2
4	308	7.4	9.3	9.6	9.0	-1.0	-0.4	2.3	2.0
5	275	13.7	18.2	18.6	16.8	14.2	16.3	18.4	17.5
6	227	-13.6	-7.0	-5.9	-7.4	5.5	9.1	10.5	9.6
7	317	-3.5	-2.0	-1.8	-2.3	-1.9	-1.3	2.9	2.6
8	229	9.6	13.6	14.0	9.9	4.6	18.4	27.5	25.6
9	243	2.7	1.0	1.8	-0.5	-11.1	2.4	6.9	5.7
10	302	6.8	9.9	9.5	8.2	-1.0	0.2	1.7	1.0
11	385	-0.2	7.6	2.3	1.6	1.6	5.0	7.0	6.7
12	265	6.9	10.2	11.8	11.0	-4.7	-3.0	-0.3	-0.7
13	385	-21.4	-14.9	-19.2	-20.1	0.3	4.7	7.0	6.3
14	235	-3.9	3.3	4.1	2.2	13.5	17.2	17.5	16.4
15	275	8.8	13.1	12.9	11.5	9.5	11.5	13.6	12.8
16	241	6.2	13.0	14.2	12.4	9.8	12.3	14.1	13.3
17	263	2.2	6.4	7.9	6.7	4.8	7.3	10.6	9.9
18	243	-2.9	2.2	2.7	1.6	-3.0	-0.4	4.3	3.7
19	263	-19.3	-15.6	-15.2	-16.4	-7.0	-5.1	-1.7	-2.4
20	279	-0.3	3.2	3.7	2.5	1.2	2.8	5.5	4.9
21	351	-2.8	4.1	2.6	1.1	3.9	6.1	8.1	7.5
22	282	3.9	6.9	6.6	5.7	-0.4	0.9	3.5	3.1
23	337	17.0	22.8	22.1	20.7	15.5	17.9	20	19.5
24	318	-7.5	-5.9	-5.8	-6.3	-0.8	-0.1	5.5	5.2
25	240	3.7	10.6	11.4	9.6	8.3	11.7	11.9	10.9
26	285	32.9	36.0	36.6	35.9	9.5	10.5	14.9	14.6
Average Percentage Overprediction		1.7	6.0	6.0	4.7	2.7	5.7	8.7	8.0
Standard Deviation (σ_n)		10.7	10.6	11	10.9	6.5	6.8	6.8	6.8
95% confidence limits									
lower		-19.2	-14.8	-15.6	-16.7	-10.0	-7.6	-4.6	-5.3
upper		22.6	26.8	27.6	26.1	15.4	19.0	22.0	21.3

TABLE 8 Inshore Wave Directions

Mean Inshore Wave Directions in degrees North

Storm No.	Wind Direction (°N)	Model OUTRAY	PCM	NPM
1	248	268	266	266
2	287	283	282	283
3	295	287	286	287
4	308	296	296	296
5	275	280	279	279
6	227	265	263	263
7	317	302	303	303
8	229	269	266	267
9	243	271	267	268
10	302	294	295	295
11	385	343	347	346
12	265	272	271	271
13	385	341	345	344
14	235	267	266	266
15	275	278	277	277
16	241	267	265	266
17	263	272	271	271
18	243	267	265	265
19	263	273	271	271
20	279	278	277	277
21	351	325	329	328
22	282	280	279	280
23	337	313	315	316
24	318	301	302	303
25	240	268	266	266
26	285	282	281	282

FIGURES.

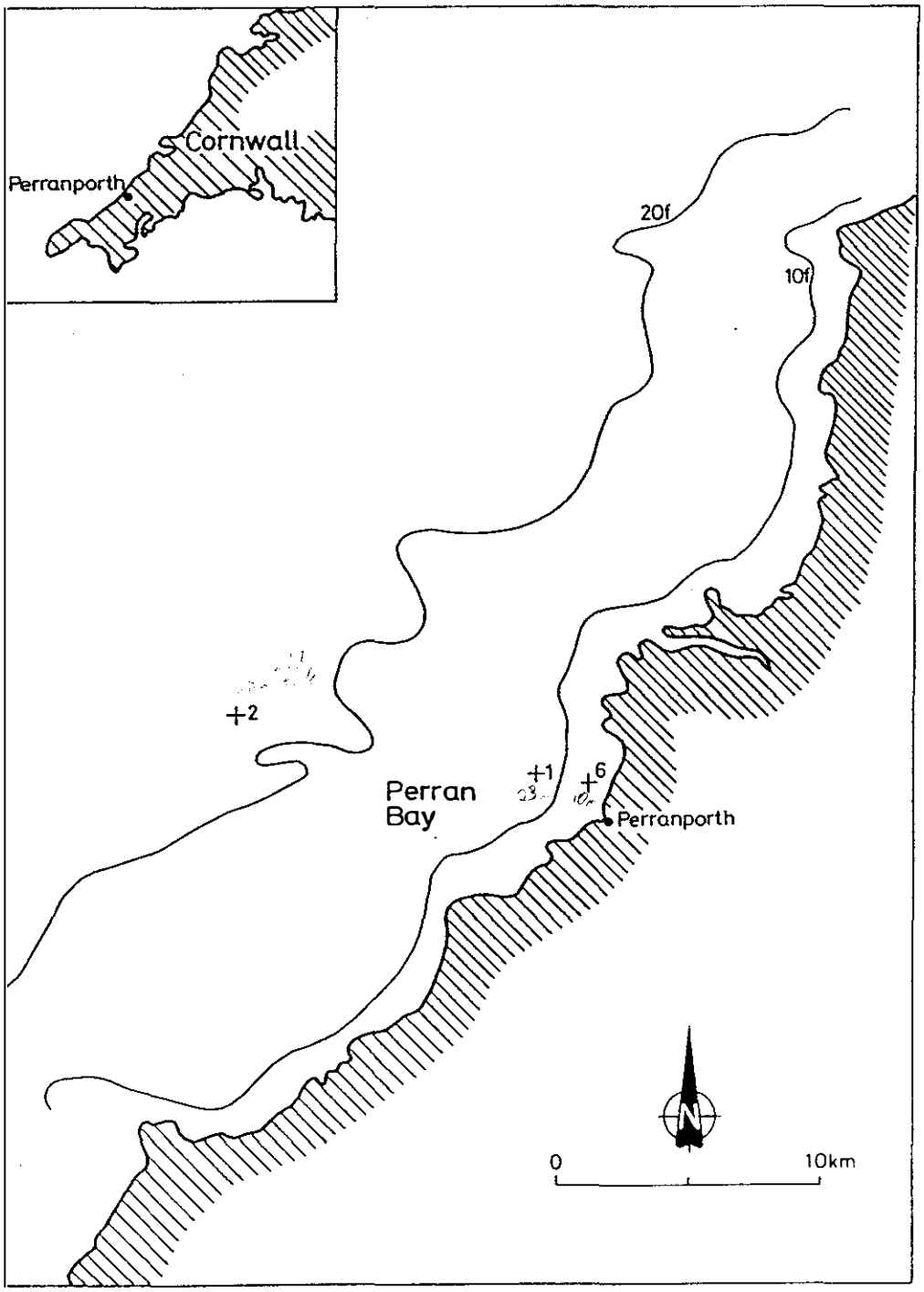

Fig 1 Location map of wave rider buoys

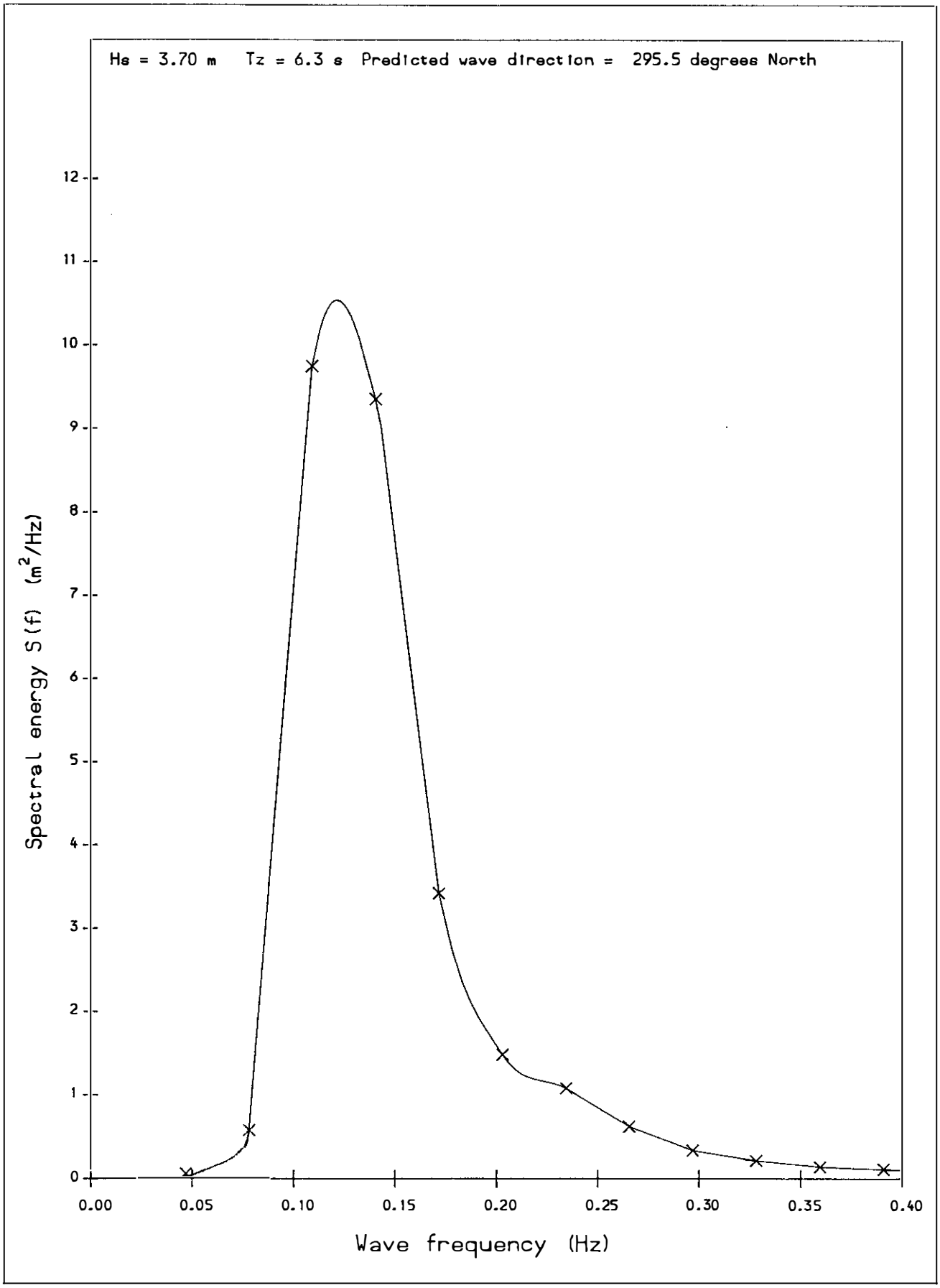

Fig 2 Offshore frequency spectrum for storm 4

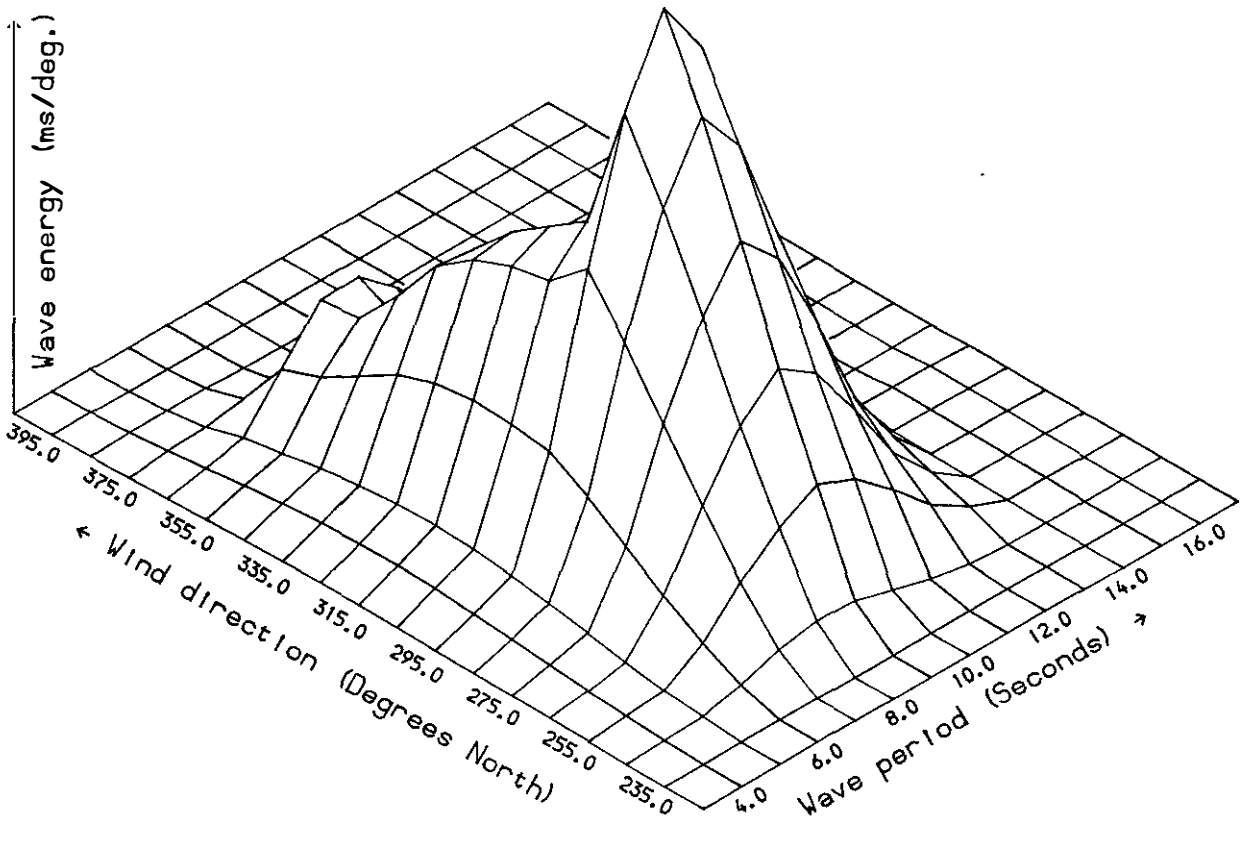

Directional wave energy spectrum

Mean wind direction 308.0 Deg. North

Hs = 3.70 Metres , Tz = 6.30 Seconds

Mean wave direction 295.5 Deg. North

Peak wave energy is 9.61 ms/deg.

Fig 3 Predicted offshore directional spectrum for storm 4

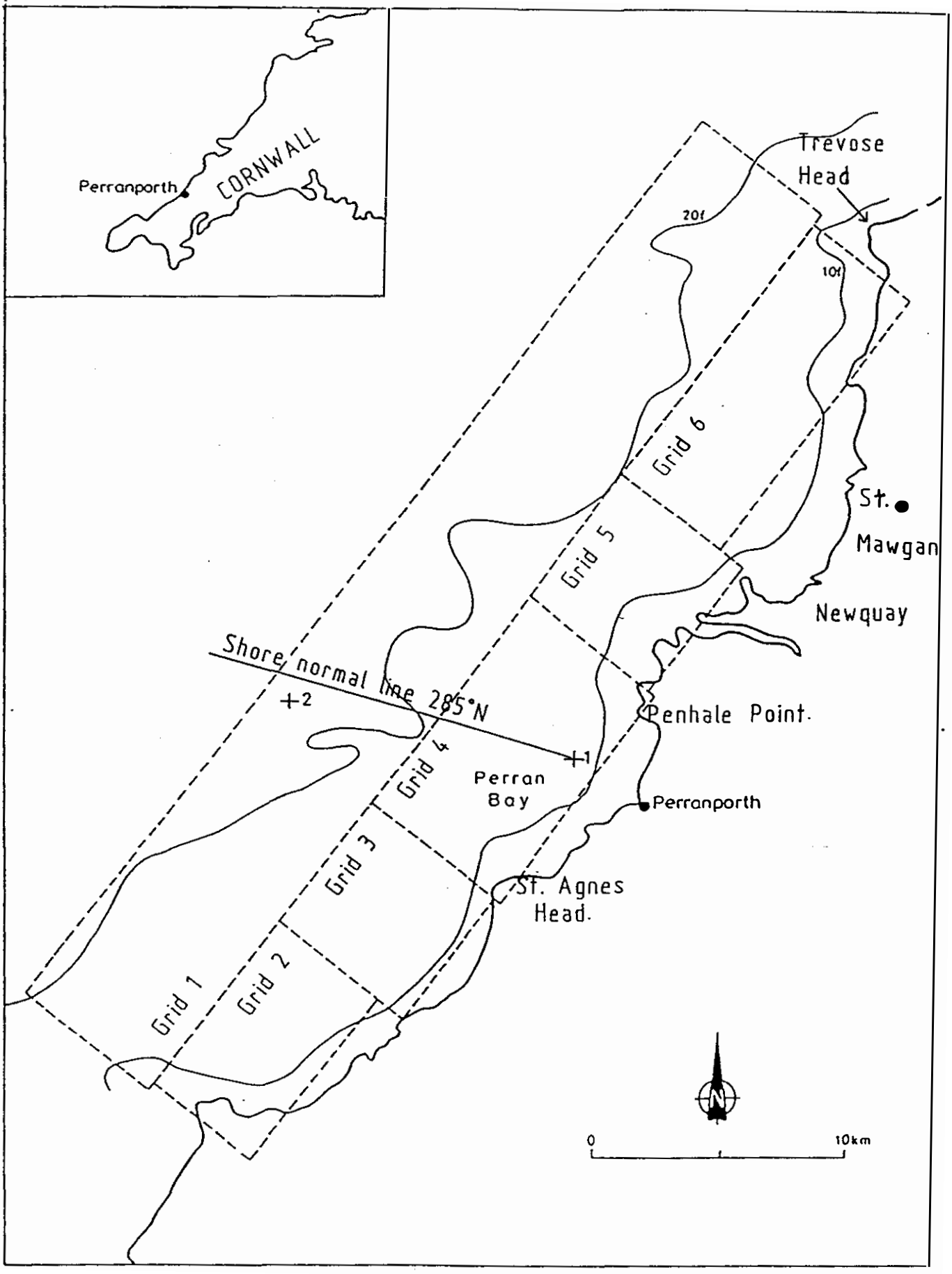

Fig 4 Location of refraction grids.

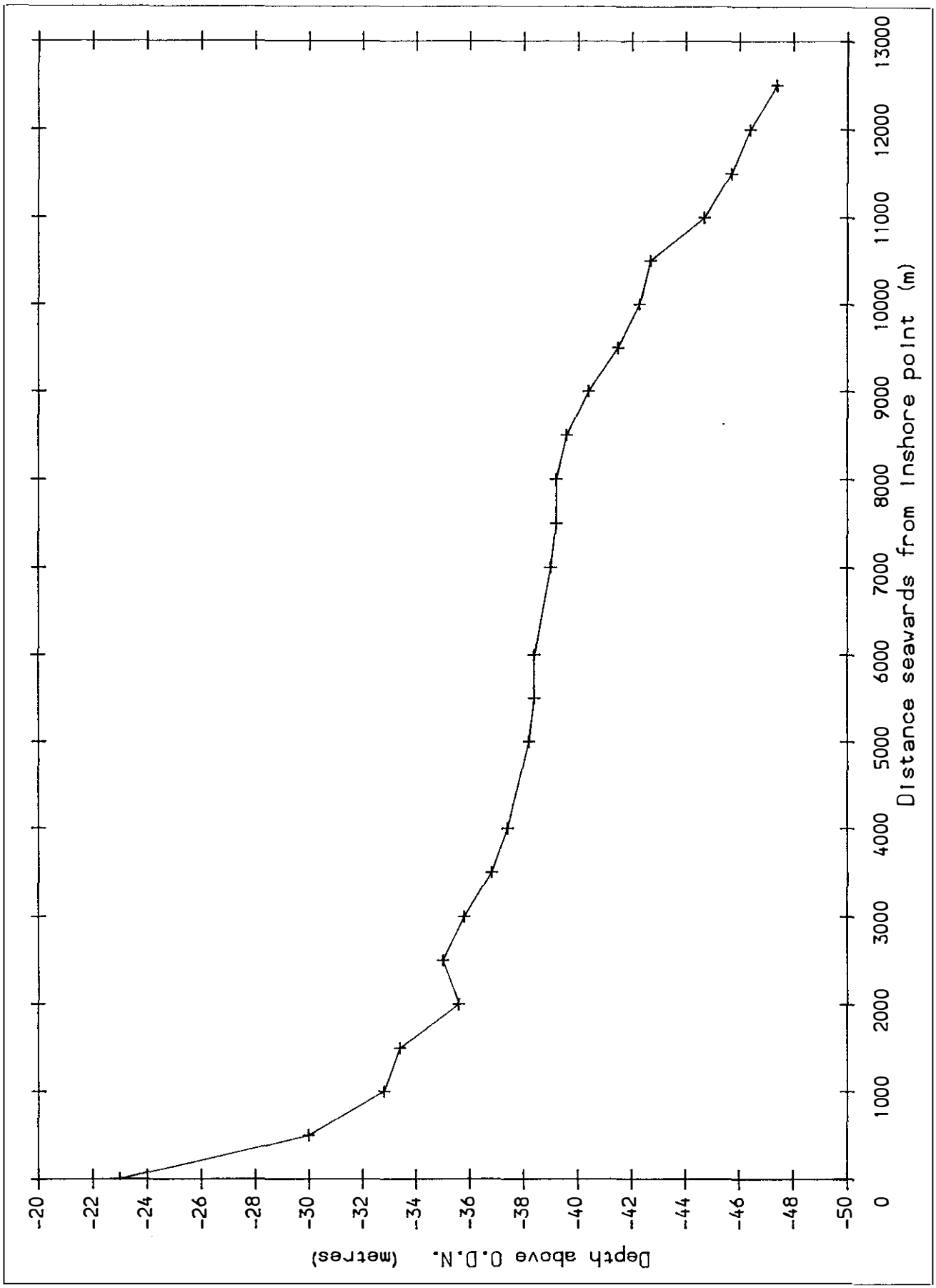

Fig 5 Depth profile used in the Nearshore Profile Model

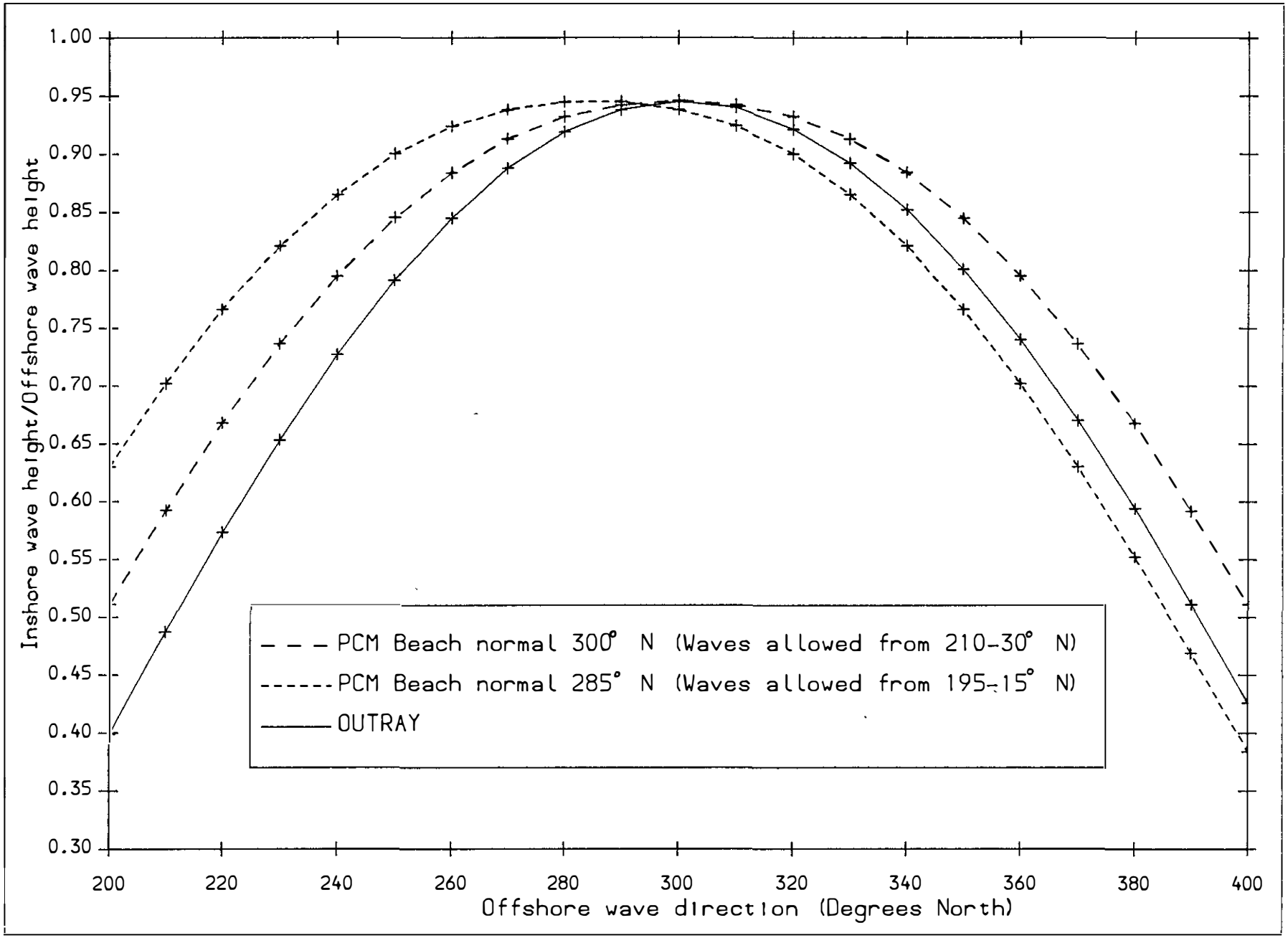

Fig 6 Wave height ratios from OUTRAY and PCM - hypothetical storm

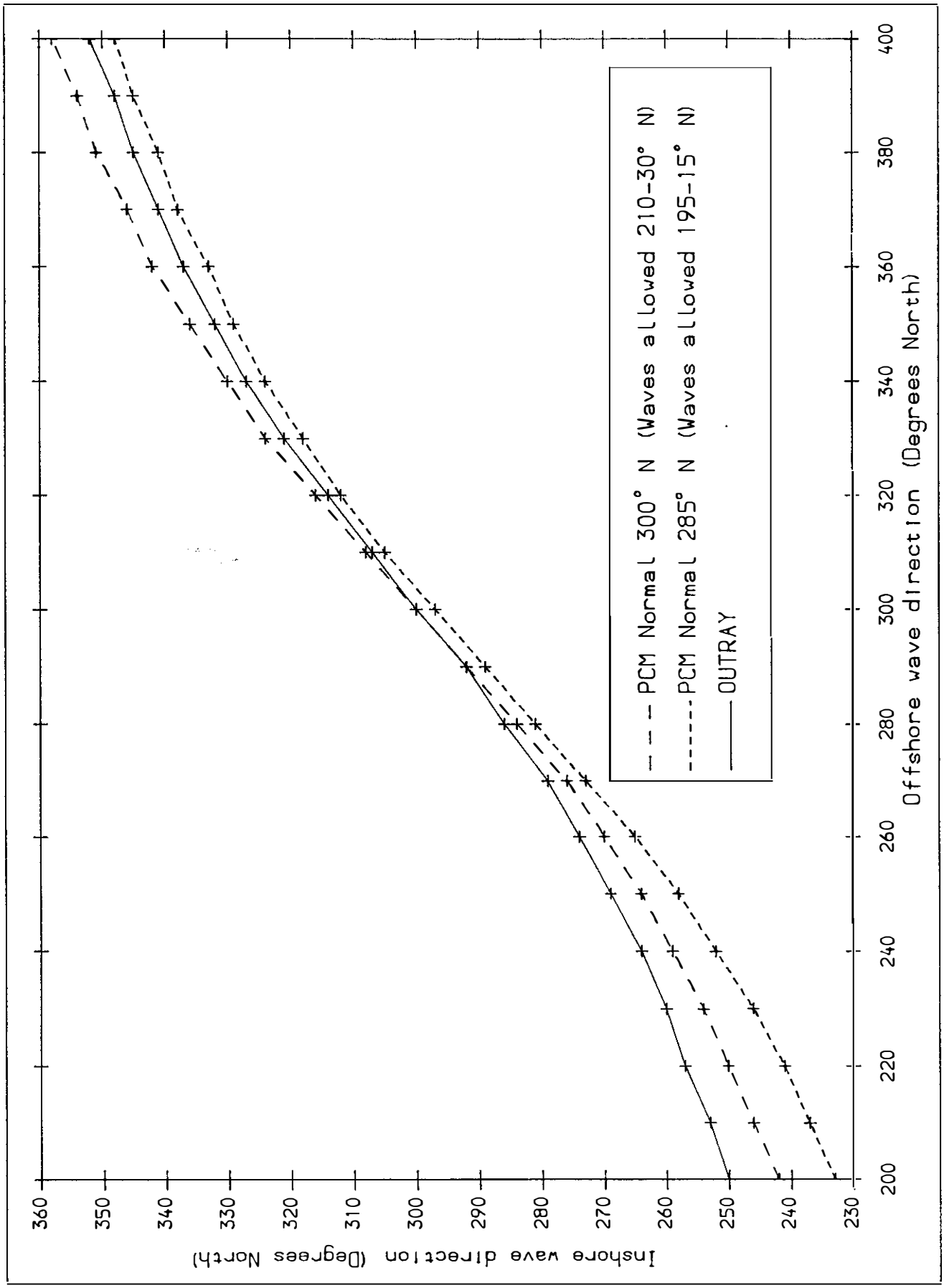

Fig 7 Wave directions from OUTRAY and PCM - hypothetical storm

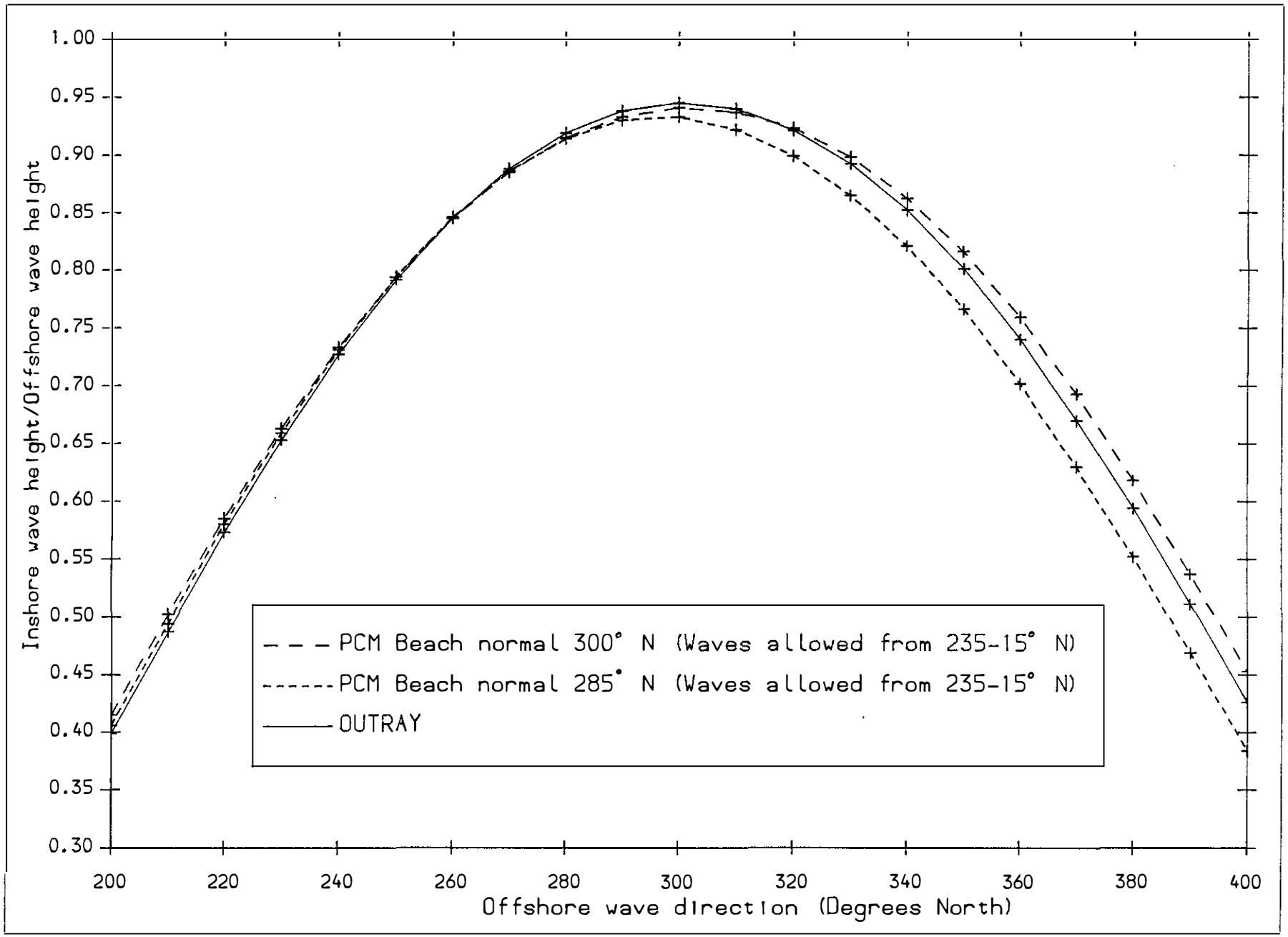

Fig 8 Wave height ratios from OUTRAY and PCM - hypothetical storm

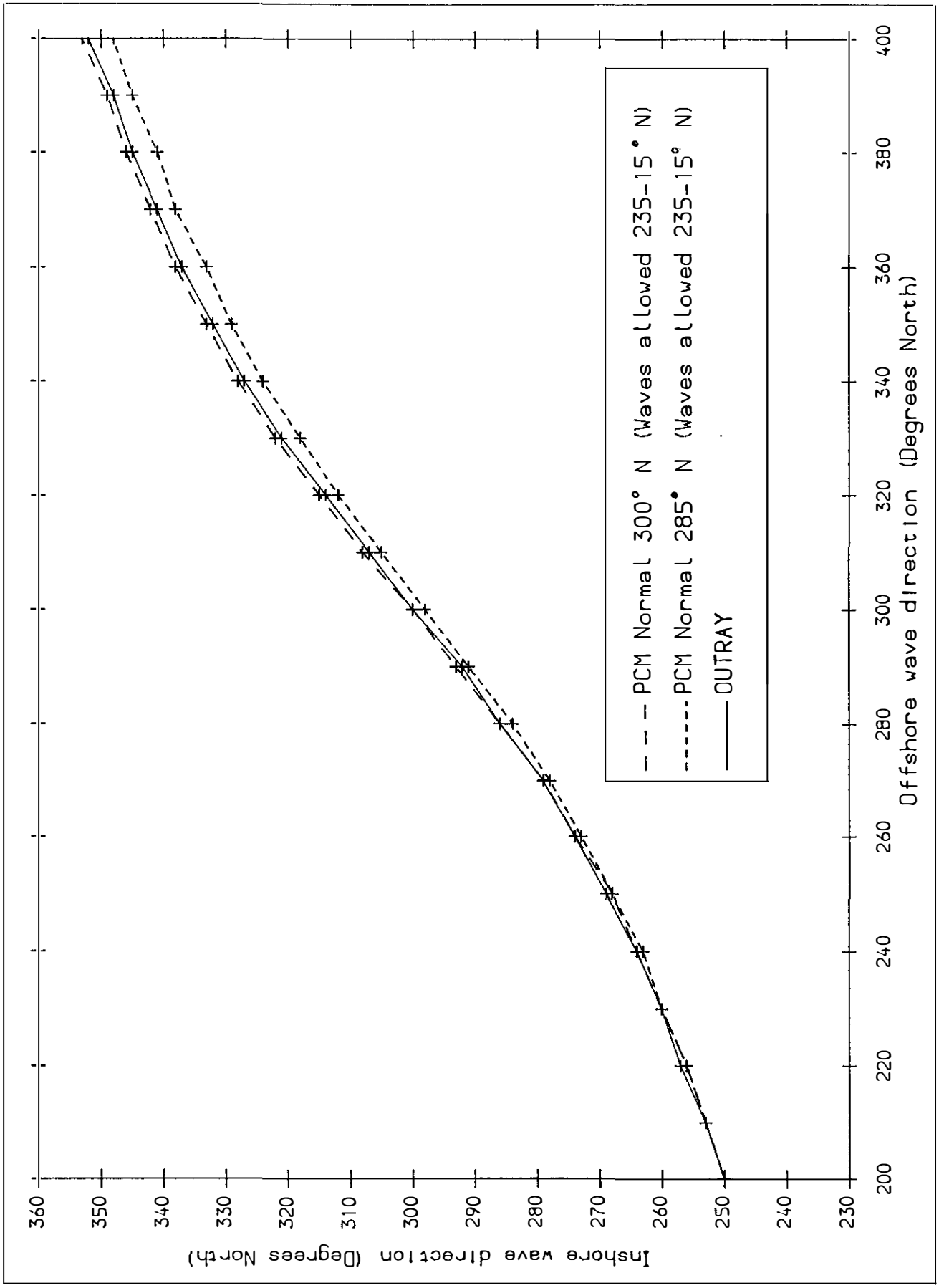

Fig 9 Wave directions from OUTRAY and PCM - hypothetical storm

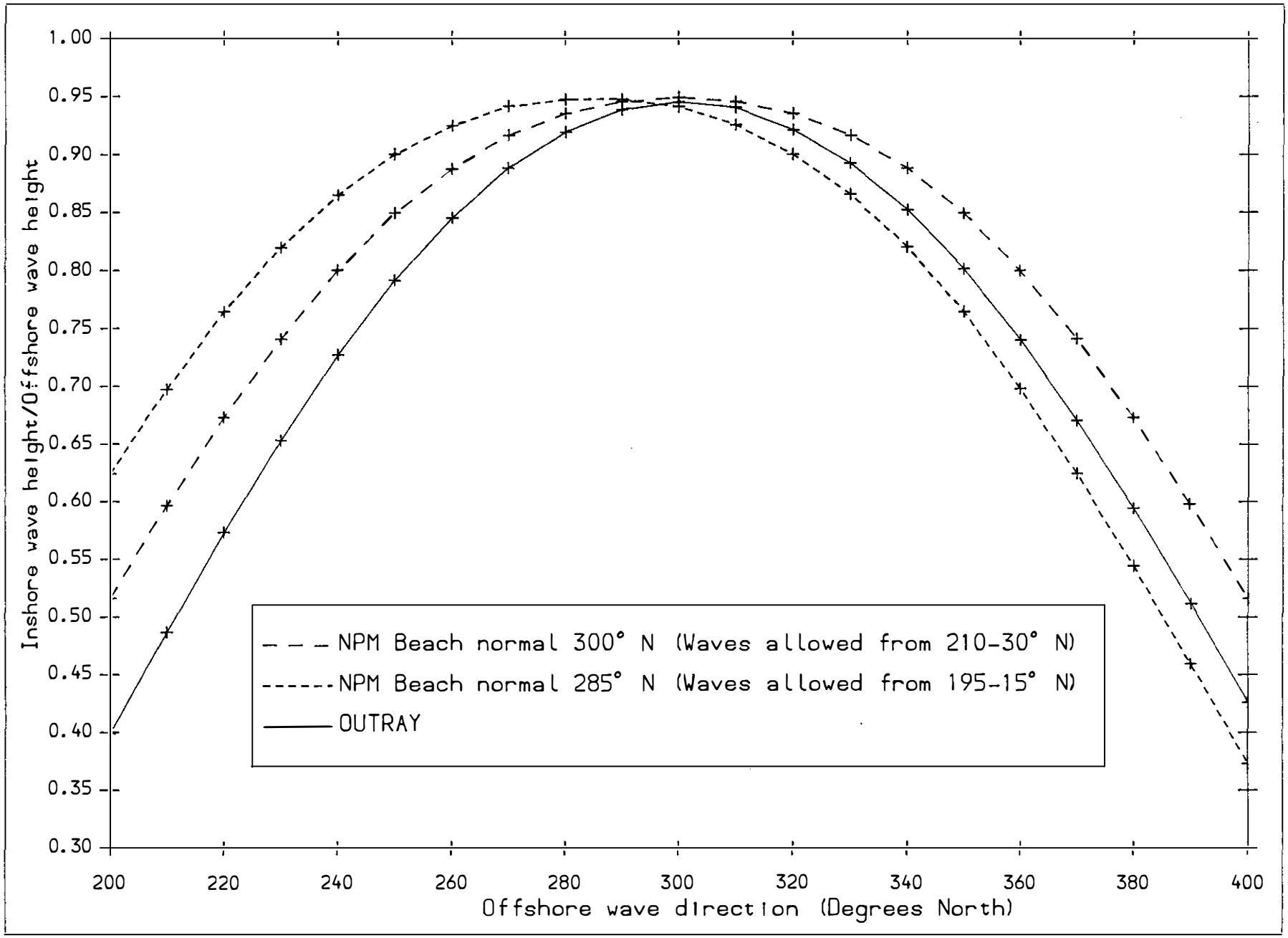

Fig 10 Wave height ratios from OUTRAY and NPM - hypothetical storm

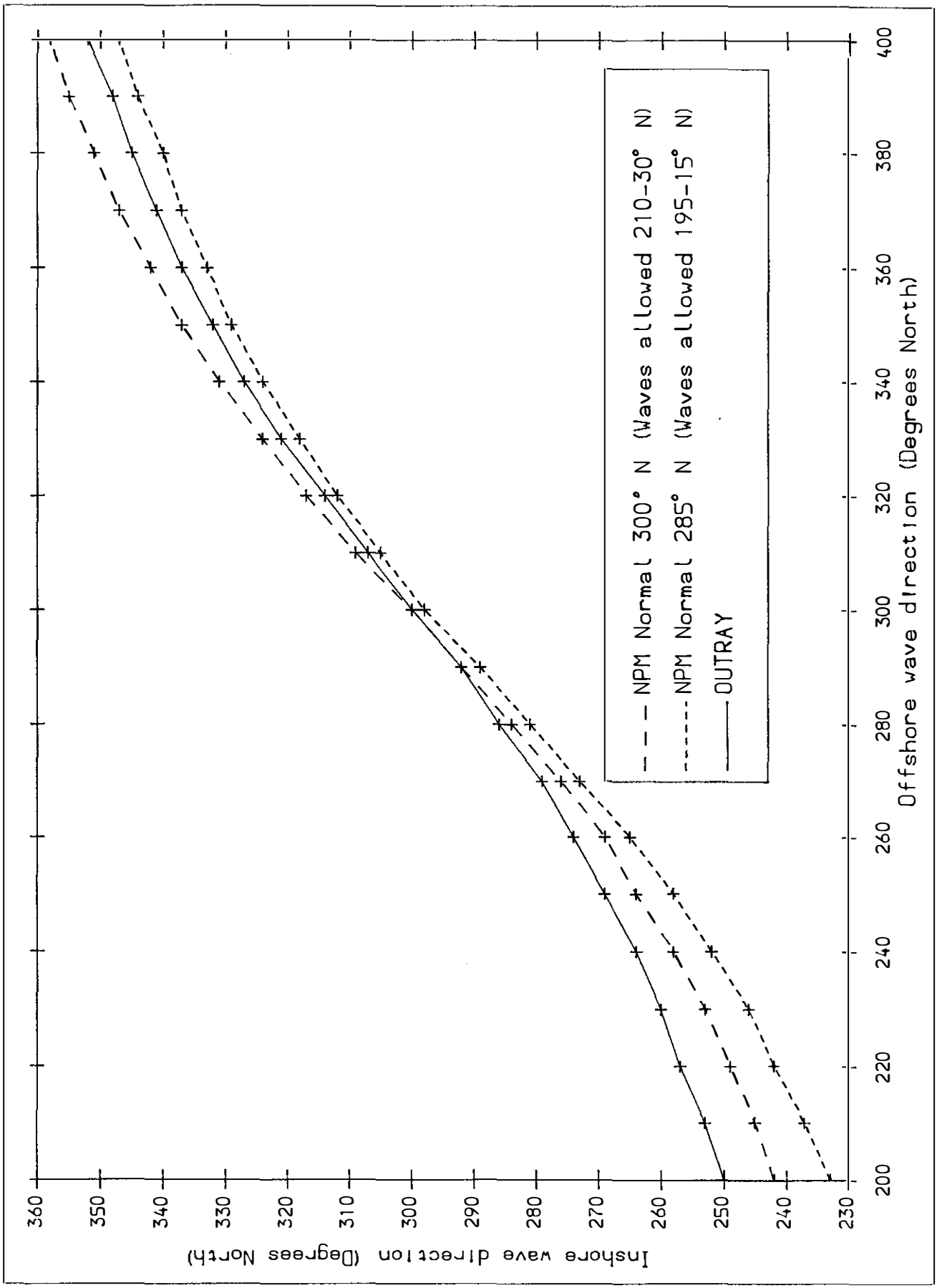

Fig 11 Wave directions from OUTRAY and NPM - hypothetical storm

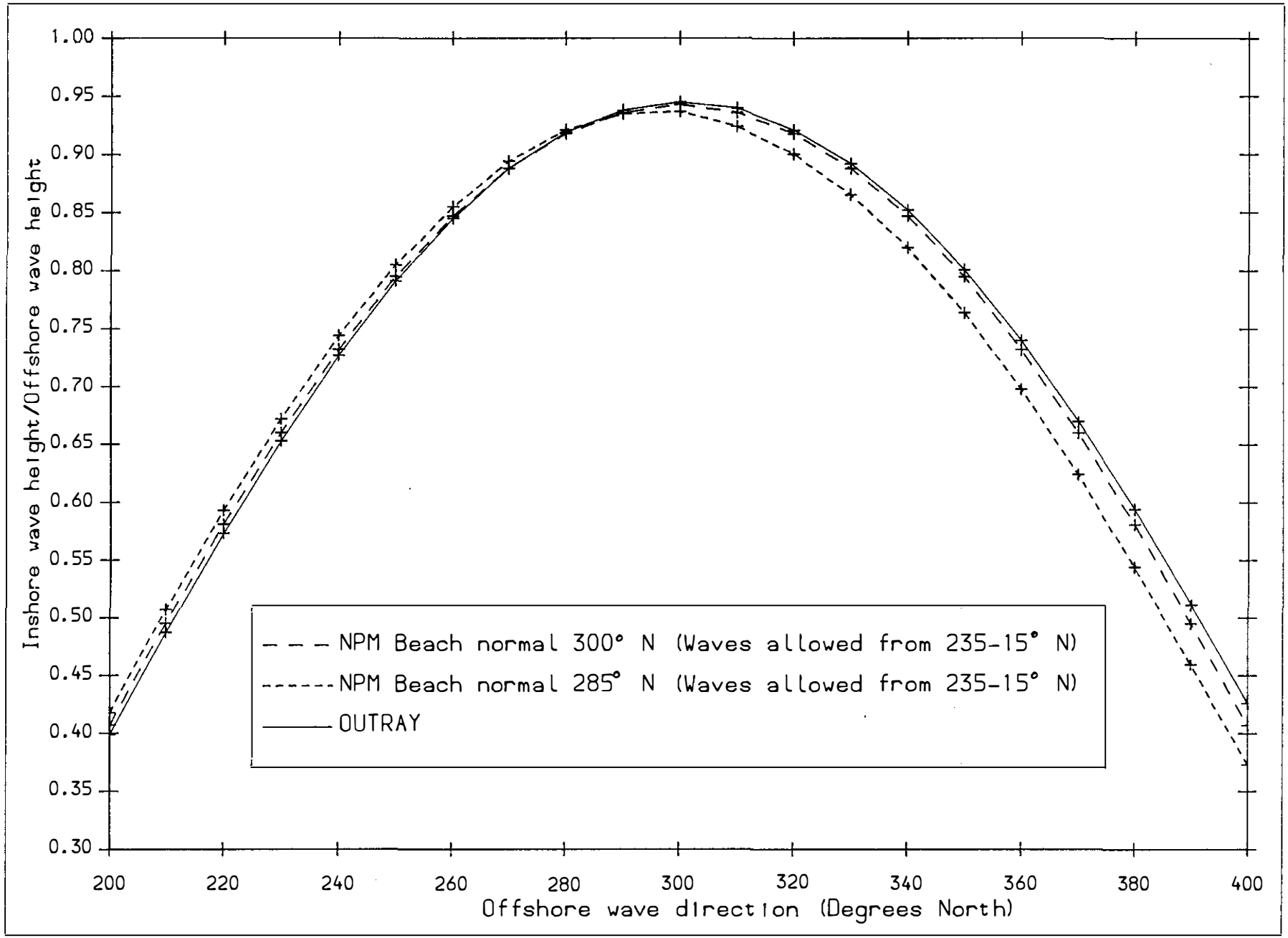

Fig 12 Wave height ratios from OUTRAY and NPM - hypothetical storm

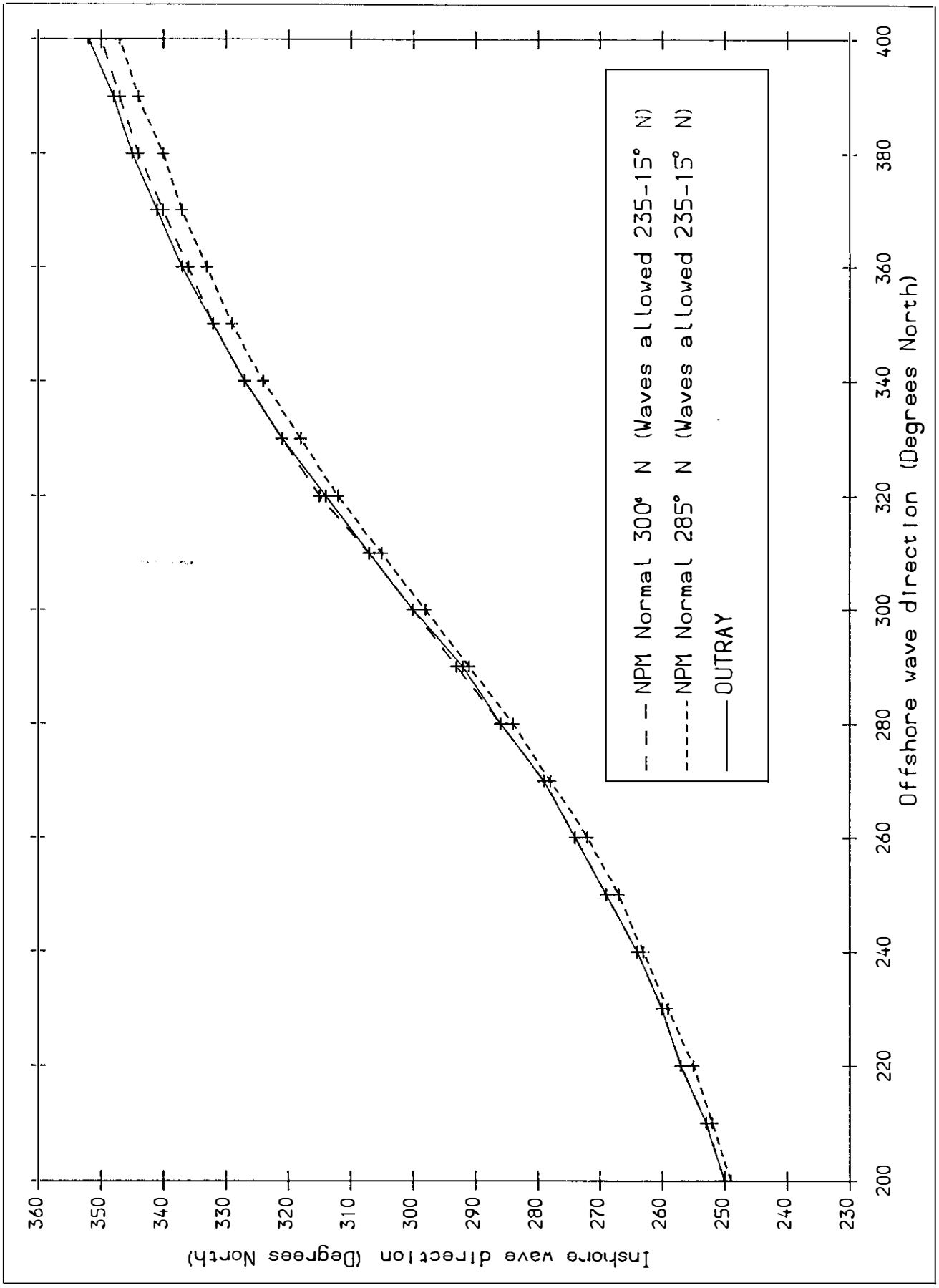

Fig 13 Wave directions from OUTRAY and NPM - hypothetical storm

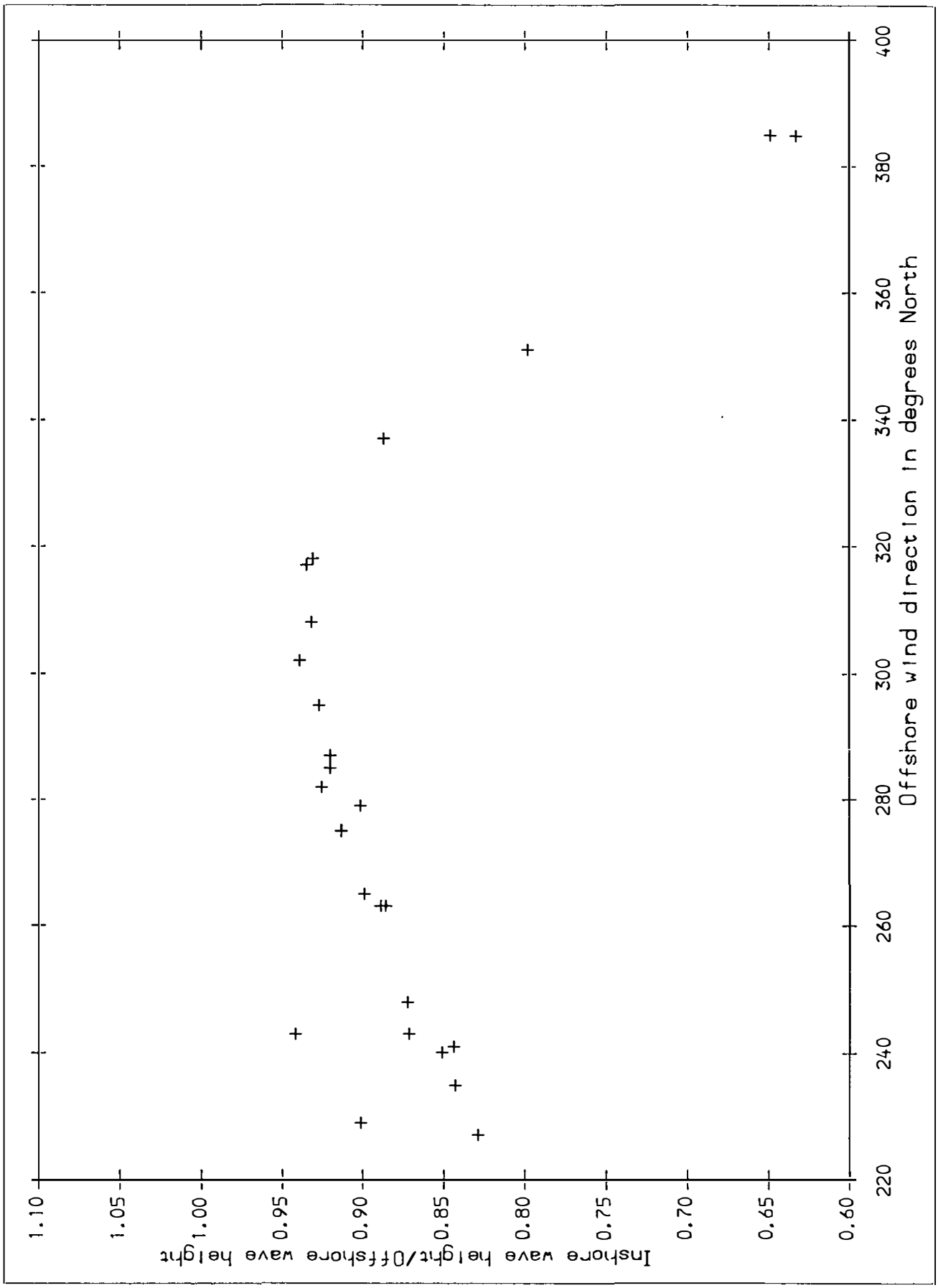

Fig 14 Wave height ratios predicted by OUTRAY

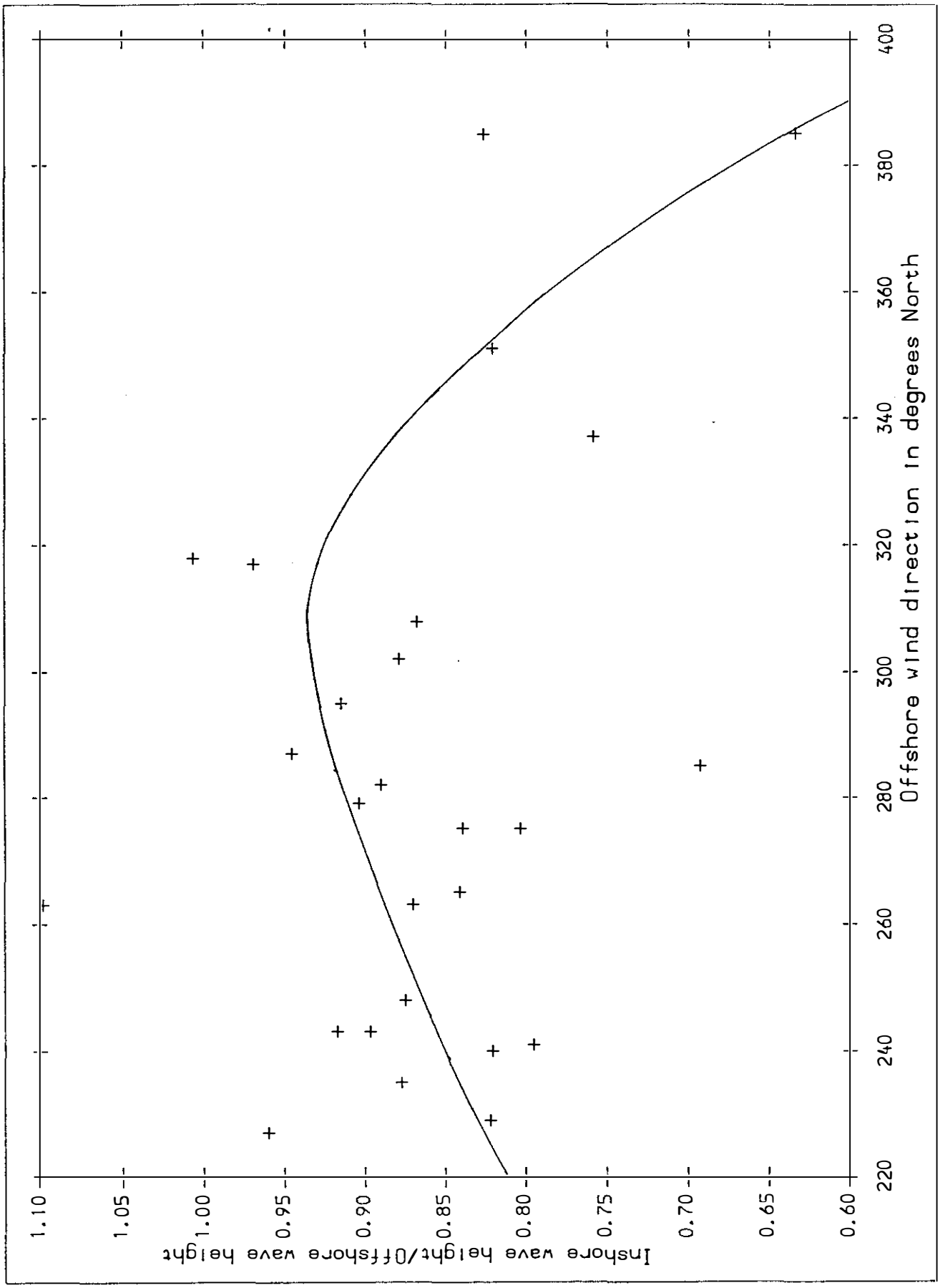

Fig 15 Wave height ratios from measured data

APPENDICES.

APPENDIX 1

The OUTRAY back-tracking refraction model

APPENDIX 1

The OUTRAY Back-tracking Refraction Model

Waves on the surface of the sea are constantly changing under the influence of a variety of external and internal forces which act simultaneously and independently. If the water is deep compared to the wavelength, the most important forces are usually the stresses resulting from wind action and internal viscosity. On the other hand, when the water becomes shallower, the effects of the seabed become increasingly important. For example, as the waves travel towards the shore they lose energy by viscous dissipation at the bed and by partial reflection, and as the water depth beneath them decreases, the waves also change direction, always tending to align their crests more nearly parallel to the contours.

This last mentioned process is known as refraction, and is similar to the refraction of light through media of different densities. The analogy can be extended further since some parts of a seabed will cause focussing of waves, whilst others will cause scattering, just as optical lenses do.

It is clear, therefore, that an accurate method of predicting wave refraction is a useful design aid when carrying out engineering studies in or beside the sea. The usual application of such a method is in predicting wave conditions at a site in shallow water, either directly or in comparison with another site. Similarly it may be used to examine changes at a site that would result from altering the seabed, for example, by dredging a channel.

In this Appendix, the Hydraulics Research method for calculating wave refraction is described.

Since the mathematical theory of wave propagation over an irregular bathymetry is far from complete, it is necessary to make simplifying assumptions and use approximate methods. Two such assumptions are made: (1) that the waves are linear, and (2) that a wave in water of local depth, d, will behave similarly to a wave in water of constant depth, d. With these restrictions it can be shown that waves progressing over a parallel contoured seabed, change their direction according to Snell's Law, i.e:

$C/\sin\alpha = \text{constant}$

where α is the angle between the wave crests and the contours and where C is the wave phase speed, a function of the wave frequency, f, and the local water depth. Since the frequency of a wave remains constant, the wave direction changes only with changing depth.

The method described, like many others, relies on the concept of wave 'rays', which are lines everywhere perpendicular to the wave crests.

In order to use Snell's Law for waves proceeding over an irregular seabed, the following method is used. A lattice of triangular cells is laid over a chart of the area of interest and depth values are read off at each intersection. In each cell the seabed is then assumed to be planar, and linear interpolation is used to define the depth at any point within the triangle. Although there is no need for the cells to be of any particular shape it is usually more convenient to choose right angled triangles which, taken in pairs, give a rectangular element.

With this representation of the seabed the depth is continuous across any grid line although the slope is

usually discontinuous. It is also possible to apply Snell's Law in each cell and to follow a wave ray across it from some given entry point and direction. As the ray leaves one cell, its position and direction become the entry conditions for its journey across the next.

The time taken to calculate the ray's path across a cell can be reduced by making a further simplifying approximation. Provided the size of each cell is small and the slope of the seabed not too steep, the wave phase speed, C, at any point inside the cell can be closely approximated by linear interpolation of the exact phase speeds at the cell vertices. The ray path, under such an assumption, is part of the arc of a circle, and the path and its direction are continuous across each grid line although the curvature of the path is usually discontinuous. Because of the simplicity of the method, there are marked advantages in cost over methods which need, for example, iterative improvements at each step or more complicated representations of the seabed topography. Rounding errors can also be expected to be smaller in the described method.

The value of a wave refraction simulation, of course, lies not in the rapidity and accuracy of calculating ray paths but in the interpretation of the information they contain. Any method based on linear theory and using the concept of wave rays cannot be expected to reproduce non-linear wave effects. In areas where the bottom topography causes strong focussing of wave rays, a situation known as a caustic, the use of linear wave theory is woefully inadequate and errors from its use will inevitably accrue. However, the method of calculating wave conditions adopted here does reduce the importance of such phenomena as caustics, and gives realistic results.

First it is assumed that in the study area a wave energy distribution $S(\theta, f, r)$ exists, where θ is the wave direction, f the wave frequency and r a position vector. In a typical open sea situation in deep water the wave energy will depend only weakly on r. On the outer boundary of the area being considered, it is thus assumed that a homogeneous sea state exists and is described by $S_o(\theta, f)$, the wave energy being considered to depend solely on direction and frequency. (The subscript o is used to denote quantities at the offshore boundary).

The purpose of the wave refraction method is to provide information on the wave conditions, or energy distribution at some point P close to the shore $S_p(\theta, f)$, for a variety of offshore conditions, ie, different values of $S_o(\theta,f)$.

Suppose a ray path exists which starts from the outer boundary of the area with direction θ_o and frequency f_n and reaches the point P with direction θ_p and frequency f_n. The functions S_o and S_p can then be linked by using a result of Longuet-Higgins (Appendix 2, Ref 1), who showed that, when expressed as a function of two perpendicular wave numbers, k_1, and k_2, the directional spectrum $S_o(k_1,k_2)$ remains constant along a ray. So using the hypothetical ray mentioned above it can be shown that

$$S_p(\theta_p,f_n) = \mu(f_n)S_o(\theta_o, f_n) \qquad \text{(A2.1)}$$

where:

$$\mu(f_n) = (C\ C_g)_o/(C\ C_g)_p \qquad \text{(A2.2)}$$

because $S(\theta, f)df\ d\theta = S(k_1,k_2)dk_1dk_2$

and $dk_1\ dk_2 = k\ dk\ d\Theta = \frac{f}{C\ C_g}\ df\ d\Theta$

where $C = \frac{f}{k}$ the phase speed

and $C_g = \frac{df}{dk}$ the group velocity of waves.

Thus we have $C\ C_g\ S(\Theta, f)$ is a constant along a wave ray, from which equation (A2.1) follows. Provided that enough rays can be found linking the outer boundary with the point P, equation (A2.1) can be used repeatedly to build up a picture of $S_p(\Theta, f)$ for any function $S_o(\Theta, f)$. All that would then be necessary are the depths at the outer boundary and the point, which would allow evaluation of C, C_g and thus $\mu(f)$.

To find such rays would be rather daunting if it were necessary to start at the outer boundary. Fortunately, however, the paths of the rays, like those in light, are completely reversible and this makes the task very simple.

Firstly a variety of wave frequencies are chosen. For a typical study these would lie in the range 0.05Hz - 0.30Hz, and about ten would be selected. Then, for each frequency a 'fan' of rays is sent out from the point of interest. Each ray is initially separated from its neighbour by a small angular increment, $\Delta\Theta_p$; for reasons of economy the smallest separation chosen is set at $\Delta\Theta_p = 0.25°$, but experience has shown that larger separations can be used for the higher frequencies without affecting the results.

Each ray is 'followed', using the method described above, until it runs ashore or reaches the outer boundary. The results from this stage of the

operation take the form of a list of those rays which connect the point to the boundary, with for each ray its frequency, f_n, its direction on leaving the point, θ_p, and its direction at the outer boundary, θ_o. Typically this list would contain information about several thousand rays.

For convenience this list is converted to three matrices which are called 'transfer functions', because they contain all the information necessary to evaluate the transfer of energy from the outer boundary to the point. Although it would be interesting to evaluate $S_p(\theta, f)$, the energy distribution at the point, completely, in most cases all that is required is an idea of the mean direction and directional spread of the waves together with the distribution of energy over frequency which will allow the derivation of a significant wave height and a significant wave period.

To obtain the energy for each frequency component, f_j, in $S_p(\theta, f)$ the angular dependence is integrated out. Equation (A2.1) thus gives

$$S_p(f_j) = \int S_p(\theta_p, f_j)d\theta_p = \mu(f_j) \int S_o(\theta_o, f_j)d\theta_p \qquad \text{(A2.3)}$$

The second integral is now replaced by a summation over all those rays followed for this frequency, and so

$$S_p(f_j) = \mu(f_j) \sum S_o(\theta_o, f_j)\Delta\theta_p \qquad \text{(A2.4)}$$

where $\Delta\theta_p$ is the angular separation used at the inshore point. This summation is now simplified as follows. It is assumed that the function $S_p(\theta_o, f_j)$, is constant over angular sectors $(\ell - 1)\Delta\theta_o$ to $\ell\Delta\theta_o$, $\ell = 1, 2, \ldots, m$, with area $A_\ell(f_j)$ in each sector.

Equation (A2.4) becomes:

$$S_p(f_j) = \mu(f_j)(\Delta\theta_p/\Delta\theta_o) \sum_{\ell=1}^{m} A_\ell(f_j) \cdot N_\ell$$

where N_ℓ is the number of rays with offshore direction between $(\ell-1)\Delta\theta_o$ and $\ell\Delta\theta_o$.

With the energy thus evaluated for all frequencies considered, ie f_j, $j = 1, 2, \ldots\ldots n$, the complete energy spectrum $S_p(f)$ has been approximated. Then, the significant wave height is defined as

$4(\int S_p(f)df)^{1/2}$ and the zero-crossing period as $(\int S_p(f).df/\int S_p(f).f^2.df)^{1/2}$.

To obtain a mean direction and angular spread for $S_p(\theta, f)$ further investigation is necessary. We define a mean vector V at the point by

$$V(f_j) = \int S_p(\theta_p, f_j)\exp(i\theta_p)d\theta_p / \int S_p(\theta_p, f_j)d\theta_p \qquad \text{(A2.5)}$$

The mean direction θ is then given by

$\theta(f_j) = ph(V(f_j))$, the phase of V_j

and the variance, or spread, $\sigma^2(f_j)$, by

$$\sigma^2(f_j) = 1 - \left|V(f_j)\right|^2$$

Following the same approximations as before, equation (A2.5) is written

$$V(f_j) = \sum_{\ell=1}^{m} \frac{A_\ell}{\Delta\theta_o} \mu(f_j) \int \exp(i\theta_p)\, d\theta_p \,/$$

$$\sum_{\ell=1}^{m} \frac{A_\ell}{\Delta\theta_o} \mu(f_j) \int d\theta_p$$

which leads to

$$V(f_j) = \sum_{\ell=1}^{m} A_\ell (U_\ell + iV_\ell) / \sum_{\ell=1}^{m} A_\ell T_\ell$$

where $U_\ell + iV_\ell = \mu(f_j) \frac{\Delta\theta_p}{\Delta\theta_o} \sum \exp(i\theta_p)$

where this summation is over all the rays with offshore angle in the range $(\ell - 1)\Delta\theta_o$ to $\ell\Delta\theta_o$.

The transfer functions are thus

$$\begin{bmatrix} T_\ell \\ U_\ell \\ V_\ell \end{bmatrix} = \mu(f_j) \frac{\Delta\theta_p}{\Delta\theta_o} \sum \begin{bmatrix} 1 \\ \cos\theta_p \\ \sin\theta_p \end{bmatrix} \qquad \text{(A2.6)}$$

where the summation is over all the rays with offshore bearings in the range $(\ell - 1)\Delta\theta_o$ to $\ell\Delta\theta_o$.

We then have

$$S_p(f_j) = \sum_{\ell=1}^{m} A_\ell T_\ell \qquad \text{(A2.7)}$$

the mean direction

$$\theta(f_j) = \tan^{-1} \left(\sum_{\ell=1}^{m} A_\ell V_\ell / \sum_{\ell=1}^{m} A_\ell U_\ell \right) \qquad \text{(A2.8)}$$

and the variance

$$\sigma^2(f_j) = 1 - [(\sum A_\ell V_\ell)^2 + (\sum A_\ell U_\ell)^2]/(\sum A_\ell T_\ell)^2 \qquad \text{(A2.9)}$$

As can be seen from equation (A2.6), the functions T, U and V can be calculated simply, using information about the ray paths. It is only for substitution into equations (A2.7), (A2.8) and (A2.9) that it is necessary to calculate the offshore spectrum S_o at each frequency f_j and angular sector $(\ell-1)\Theta_o$ to $\Delta\Theta_o$ to give A_ℓ.

Thus for one set of wave rays, and consequently one set of transfer functions, wave conditions at the inshore point can be calculated for a large variety of functions $S_o(\Theta, f)$. The only restrictions on the offshore spectra that can be used are that they vary sufficiently slowly with Θ_o that they can be assumed constant over angular sectors of width $\Delta\Theta_o$ and that the frequencies f_j enable an accurate representation of the energy distribution over frequency. In practice, of course, the offshore spectra are chosen first and the quantities $\Delta\Theta_o$ and f_j are then chosen to satisfy these restrictions.

Appendix

References

1. LONGUET-HIGGINS M S. The transformation of a continuous spectrum by refraction. Proc. Camb. Phil Soc, No 1, 1957, pp226 - 229.

APPENDIX 2

The HINDWAVE wave hindcasting model

APPENDIX 2

The HINDWAVE Wave Hindcasting Model

The HINDWAVE model

The HINDWAVE model (Ref 1) has been developed at HR, for prediction of wave climate at coastal locations, based on wind records for the area. It has been used successfully on many projects at various sites around the British coast.

The computations are split into two main parts. The first stage consists of production of a menu (or list) of about one thousand possible wave conditions, from a similar number of specific wind conditions. Fetch or open water rays are measured at 10° intervals around the wave prediction point for use as input to the first element of HINDWAVE, ie the JONSEY wave generation sub-model described in Section 2 of this Appendix. The second part consists of analysis of wind records. For each hour in the sequence, the wind/wave condition most closely corresponding to actual wind activity at that time is chosen from the menu. The analysis works with measured wind data collected at hourly intervals over a period of several years. The wave conditions at any time are estimated with regard to wind speeds during the preceding day or so.

It is first necessary to define a few standard terms used in wave prediction and analysis. Significant wave height (H_s) is a parameter in common use among coastal engineers as a means of expressing wave severity. It equates to the average height of the highest one third of the waves in a sequence. Wave period is usually indicated by either mean zero-crossing period (T_z), or peak period (T_p) at which the wave energy spectrum is densest. Direction can be expressed as either wind direction (θ), or the

mean wave direction (Θ_w) averaged over all frequency and direction components.

The JONSEY program is used to assign a particular H_s, T_p and Θ_w to each member of a particular set of wind conditions. The set comprises all possible combinations of sufficient values of speed, direction and duration to cover the range of values expected at that location. The predicted heights, periods and directions are stored for use as a look-up table. The technique described here is to break down the measured wind data into discrete categories, and then to select the corresponding H_s, T_p and Θ_w from the table.

The first stage in the procedure is to select which wind conditions could occur and to divide them into discrete bands in terms of wind speed, direction and duration. The corresponding predicted H_s, T_p and Θ_w values are calculated and retained.

If the wind speed remains steady over a long period, a twenty-four hour or even longer generation time is likely to be appropriate for exposed sites. However, if the wind speed or direction is rapidly varying, a shorter duration will be used as input to the wave prediction equations. The method of selecting the duration, wind speed and wind direction for each hour, is explained below.

Hourly wind speeds and directions are obtained from the Meteorological Office in the form of a computer data file. For each hour in turn, the method determines, for the chosen group of durations, the dominant set of wind conditions at the prediction location, with reference to the H_s table. This is achieved by vectorially averaging the wind velocities over the various chosen durations leading up to that time in order to obtain an average speed and direction

for each. The largest value is then selected from the corresponding set of H_s levels. This figure is retained together with the appropriate peak period and wave direction, in order to build up a probability distribution for each month.

A further option is automatic extrapolation to extreme wave heights, for different direction sectors, based on the overall predicted distribution of H_s. This is done by fitting a three-parameter Weibull distribution to the data in each direction sector in turn, after which the results are tabulated for various return periods.

The JONSWAP/SEYMOUR wave prediction model

It is observed that wind-generated waves show some directional spreading about their mean direction of propagation. Wind travelling over a water surface transmits energy to the water in directions on either side of its own direction, which may fluctuate during the period of wave generation.

To incorporate this effect in the model, components of the total wave directional spectrum are calculated for various directions either side of the mean, and then a weighted average is taken using a standard spreading function. The significant wave height, period and direction are then calculated at the target point, by numerical integration of the spectrum.

The component directions (i = 1 to n) are spaced at regular intervals ($\Delta\Theta$) in the range ±90° from the mean (Θ_o). For each one (Θ_i), the mean JONSWAP equation (Ref 2), representing a growing wind sea, is used to define the spectrum (E_i), given as a function of frequency (f):

$$E_i(f) = \alpha g^2 (2\pi)^{-4} f^{-5} \exp\{-1.25 (f/f_m)^{-4}\} \gamma^{\eta} \quad (1)$$

where:

$$\alpha = 0.032\ (f_m\ U/g)^{2.3}$$

$$\gamma = 3.3$$

$$\eta = \exp\ \{\frac{-\ (f\ -\ f_m)^2}{2\ f_m^2\ \sigma^2}\}$$

$$\sigma = 0.07 \text{ for } f \leq f_m$$
$$0.09 \text{ for } f \geq f_m$$

f_m = the peak frequency (Hz)
$= 2.84 g^{0.7}\ F^{-0.3}\ U^{-0.4}$

U = the windspeed (ms^{-1})

F = the fetch (m) (fetch-limited conditions)
$= 0.008515 t^{1.298} g^{0.298} U^{0.702}$ (duration-limited)

g = the acceleration due to gravity (ms^{-2})

t = the duration (s)

The summation of the component spectra is then performed using the Seymour equation (Ref 3), which includes the cosine-squared directional spreading function for a directional wave spectrum ($E(f,\Theta)$). It is applied in the range ±90° from the principle wind direction. If the fetches are measured at say 10° intervals ($\Delta\Theta$), then the effective wave spectrum (E) for a particular direction (Θ_0) is calculated as the weighted average for seventeen component spectra ($E_i(\Theta_i)$, Θ_i = -80°, -70°, ..., 80° for i = 1, 17), as indicated in equation (2).

$$E = (2\Delta\Theta/\pi) \sum_{i=1}^{17} E_i \cos^2(\Theta_i - \Theta_0) \qquad (2)$$

Although it is not part of the original theory, experience at HR indicates that cosine-sixth is sometimes a better spreading function to use. This is particularly true when the wave generation area is unusually narrow or the peak period is unusually long. In order to use this modification, the cosine term in equation (2) is raised to the power six rather than two, and the coefficient $2/\pi$ is increased to $3.2/\pi$.

The significant wave height (H_s) is the average height of the largest one third of the waves. The mean zero-upcrossing period (T_z) is the period measure most frequently used in engineering, this being the average time between successive upcrossings of the mean level by the water surface. The mean wave direction (Θ_w) is taken as the average of the spectral components over all frequencies and directions. They are all approximated by numerical integration of equation (2).

$$H_s = 4m_0^{1/2} \qquad (3)$$

$$T_z = (m_0/m_2)^{1/2} \qquad (4)$$

$$\Theta_w = \Theta_0 + \frac{\int\int E(f,\Theta)(\Theta - \Theta_0)\,df\,d\Theta}{\int\int E(f,\Theta)\,df\,d\Theta} \qquad (5)$$

where $m_n = \int E(f)\, f^n df$

In order to use this method, fetch lengths must be known over a range of at least 180° around a point. It is convenient to use discrete frequencies in equations (1) and (2) which should also be specified.

For each application of the method, a duration and a fetch are given, although only one or other of these will produce the limiting condition used in equation (1). A complete directional spectrum is calculated, from which is obtained the one-dimensional spectrum as well as H_s, T_z and Θ_w.

The directional spread of the predicted wave spectrum will generally be frequency dependent. The cosine-squared function is applied to component spectra, which are generated over different fetch lengths, and which will consequently have different total energies and different peak frequencies. This has the following realistic effect upon the calculated directional spread of energy. If the wind direction corresponds to one of the long fetch directions, then the spreading of energy at the peak will be lower than average, whilst more spreading will be observed at the highest frequencies. If the wind is blowing along one of the shorter fetches, then the spread will tend to be more even across different frequencies, and in an extreme case, may produce greater than average spreading at lower frequencies.

Appendix

References

1. Hawkes P J. A wave hindcasting method. Conference on modelling the offshore environment, Society for Underwater Technology, April 1987.

2. Hasselmann K et al. Measurements of wind wave growth, swell and decay during the Joint North Sea Wave Project (JONSWAP). Deutsches Hydrographisches Institute, Hamburg, 1973.

3. Seymour R J. Estimating wave generation on restricted fetches. Proc ASCE, Vol 103, No WW2, May 1977.